ANALYSIS OF PASSIVE ACOUSTIC RANGING OF HELICOPTERS FROM THE JOINT ACOUSTIC PROPAGATION EXPERIMENT

5/3-71
201685
P- 40

Benny L. Carnes
John C. Morgan

U.S. Army Engineer Waterways Experiment Station
Vicksburg, Mississippi

PREFACE

The study reported herein was conducted by the U.S. Army Engineer Waterways Experiment Station (WES), Vicksburg, Mississippi, during fiscal year 1993. It was funded by WES under the Laboratory Discretionary Research Program.

This study was conducted under the general supervision of Mr. Bryant Mather, Director of the Structures Laboratory (SL), WES, and Mr. L. K. Davis, Chief of the Explosion Effects Division (EED), SL, and under the direct supervision of Dr. Benny L. Carnes, Acoustic/Seismic Research Team Leader and Project Coordinator, SL.

This report was prepared by Dr. Carnes and Mr. John C. Morgan, assigned to WES from the Illinois Institute of Technology Research Institute, Dayton, OH, office. Field data acquisition was conducted by Messrs. Larsen and Leo Koestler of the WES Instrumentation Services Division. Data analysis and preparation were performed by Messrs. Morgan and Travis Harrell, assigned to WES from the Atlantic Research Corporation. A significant contribution was made in the theoretical physics by Mr. John S. Furey, assigned to WES from the Atlantic Research Corporation.

At the time of publication of this report, Director of WES was Dr. Robert W. Whalin. The Commander was COL. Leonard G. Hassell, EN.

Contents

Preface

List of Figures

Title

List of Tables

Title

134

INTRODUCTION

For more than twenty years, personnel of the U.S.A.E. Waterways Experiment Station (WES) have been performing research dealing with the application of sensors for detection of military targets. The WES research has included the use of seismic, acoustic, magnetic, and other sensors to detect, track, and classify military ground targets. Most of the WES research has been oriented toward the employment of such sensors in a passive mode. Techniques for passive detection are of particular interest in the Army because of the advantages over active detection. Passive detection methods are not susceptible to interception, detection, jamming, or location of the source by the threat. A decided advantage for using acoustic and seismic sensors for detection in tactical situations is the non-line-of-sight capability; i.e., detection of low flying helicopters at long distances without visual contact. This study was conducted to analyze the passive acoustic ranging (PAR) concept (previously developed at WES[1]) using a more extensive data set from the Joint Acoustic Propagation Experiment (JAPE).

Background

The PAR concept exploits the repetitive nature of helicopter acoustic signatures to compute the range and velocity of a passing helicopter. The PAR method analyzes the change of the frequency of the signatures through time, known as the Doppler shift, and calculates these parameters using the Doppler shift equations on the signals as the helicopter passes through the closest point of approach (CPA). In the previously mentioned research, the basic equations governing the extraction of range and velocity for the PAR concept were presented. The PAR concept was used on one set of data for one helicopter at one site, and it produced promising results.

Objective

The objective of this research was to investigate constraints on the PAR concept to estimate the limitations of realistic operation under various environmental conditions, and to determine if the PAR concept will apply to multiple helicopters.

ANALYSIS OF PASSIVE ACOUSTIC RANGING (PAR)

In the previous WES investigation the equations governing the behavior of the Doppler shift as a function of velocity and range were presented. The scenario of a helicopter passing an acoustic sensor is shown in Figure 1. The time that the signal is received at the sensor, t_r, is equal to the time that it is emitted, t_e, plus the time of travel. If the emitting source travels with constant velocity, v, through CPA (see figure 1) then t_e, expressed as a function of t_r, is

$$t_e - t_{cpa} = t_r - t_{cpa} - \frac{\sqrt{\beta^2 (t_r - t_{cpa})^2 + (1 - \beta^2) \rho^2}}{1 - \beta^2} \qquad (1)$$

where β is the velocity of the source divided by the speed of propagation of the signal in the media and ρ is the CPA distance divided by the speed of propagation.

The general Doppler shift formula is

$$f_r = f_e \frac{dt_e}{dt_r} \qquad (2)$$

which for the case under consideration, expressed in relevant kinematic parameters, is

$$\frac{dt_e}{dt_r} = \frac{(1 - \beta \sigma)}{(1 - \beta^2)}$$

where

$$\sigma = \frac{\beta (t_r - t_{cpa})}{\sqrt{\beta^2 (t_r - t_{cpa})^2 + (1 - \beta^2) \rho^2}} \qquad (3)$$

The Doppler shift is shown in figure 2 for various values of these parameters.

Inherent Errors

The basic method for the extraction of kinematic information from these time traces was to transform the time trace into the frequency domain. The sources had stable characteristic frequencies, which facilitated the extraction of the incoming and outgoing frequencies from these data. The velocity and fundamental frequency of the source were then computed, and frequency information as a function of time was obtained from transforms of selected windows of the time trace. As done in the previous study, these data were then used to determine the range by fitting
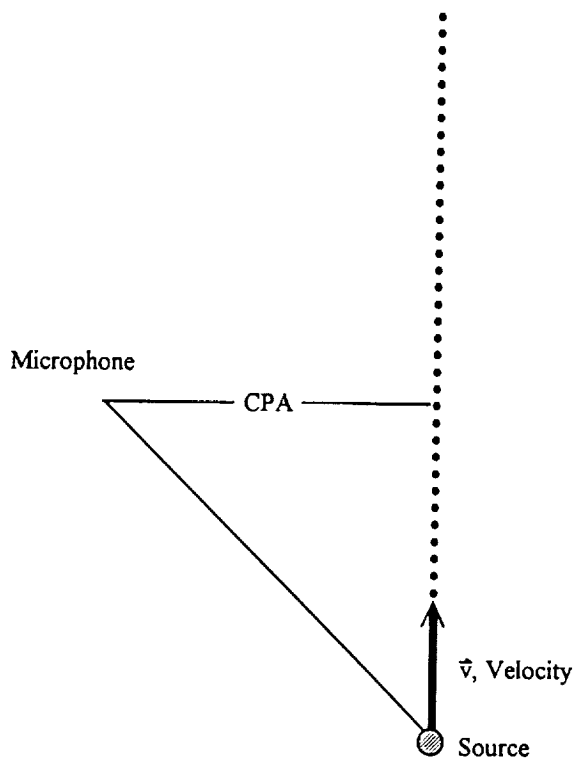
Figure 1. Diagram of source approaching a microphone.
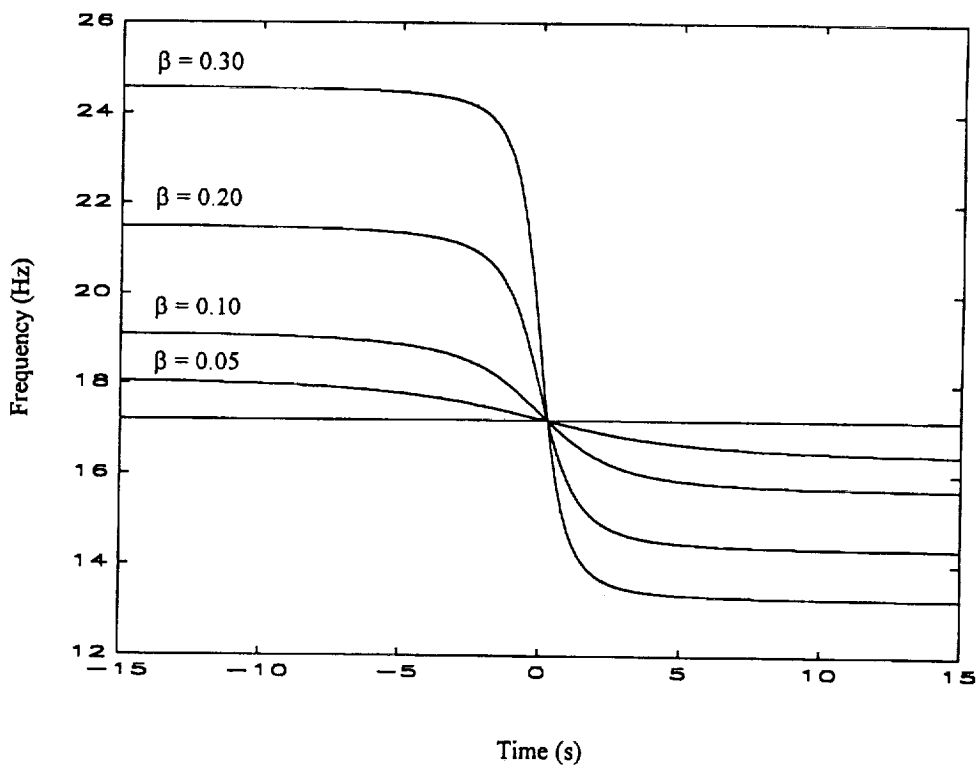
Figure 2. Plot of frequency vs time of a source with fundamental frequency of 17.2 Hz at a range of 100 m for beta=0.05,0.1,0.2,and 0.3.

137

the slope of the frequency versus time curve at CPA to the following:

$$\frac{df_e}{df_r} = \frac{-\beta\ f_e}{\rho} \tag{4}$$

The key to this operation is the transformation from the time to the frequency domain because of the spreading of the data points through the Doppler shift. Since the slope of the curve is largest at CPA, the spacing of the individual points is sparsest in that region (as can be seen in figure 3). The accuracy of the slope calculation is dependent on the size of the time step of each window.

The usual approach used to produce a data set with frequency as a function of time from a time trace is to extract sections of the time trace and perform a fast Fourier transform (FFT) on each of these sections. The problem with the FFT method is that as the length, Δt, of the sections gets smaller, the resolution, Δf, of the frequency grows larger, since

$$\Delta f = 1 / \Delta t \tag{5}$$

In addition, there is an error that is inherent to the range calculation associated with the time step. Figure 4 contains graphs of range error as a function of time step for several values of velocity and range. It can be seen from these graphs that there are cases where this error is at a minimum when the time step is the smallest value. Large changes in the other kinematic parameters affect the error to a lesser extent. Several methods were tested in an attempt to overcome this basic problem.

Processing Methods

The two most successful processing methods were the cross spectral density (CSD) method and the method of successive differences (SD).

Cross Spectral Density

The CSD method which was initially proposed for this purpose in the previous study utilizes a phase analysis of the FFT of the signal to calculate the frequency of the signal. The FFT's of successive intervals are compared by conjugation and multiplication. For a pure frequency this method can give accurate results, but because of the nature of the FFT calculation,

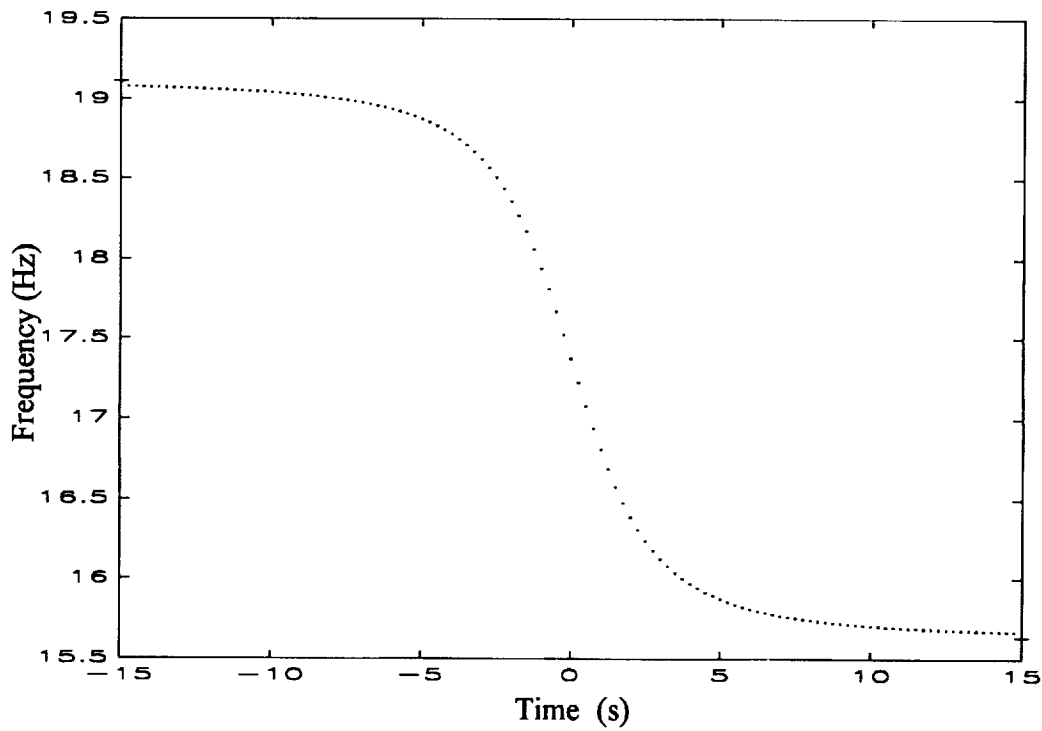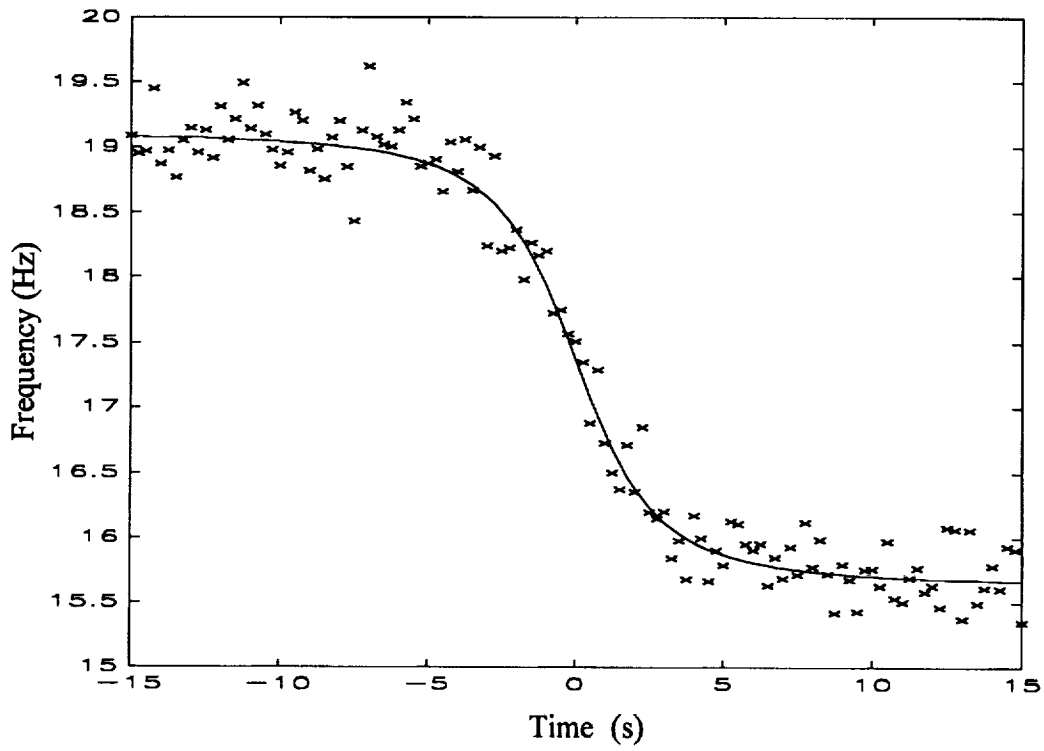Figure 3. Discrete plot of frequency values for a time step of 0.25 sec with CPA at t=0 seconds. Note the spacing of the of the points near CPA. Top shows real data and fit, and the bottom shows an example of the ideal case.
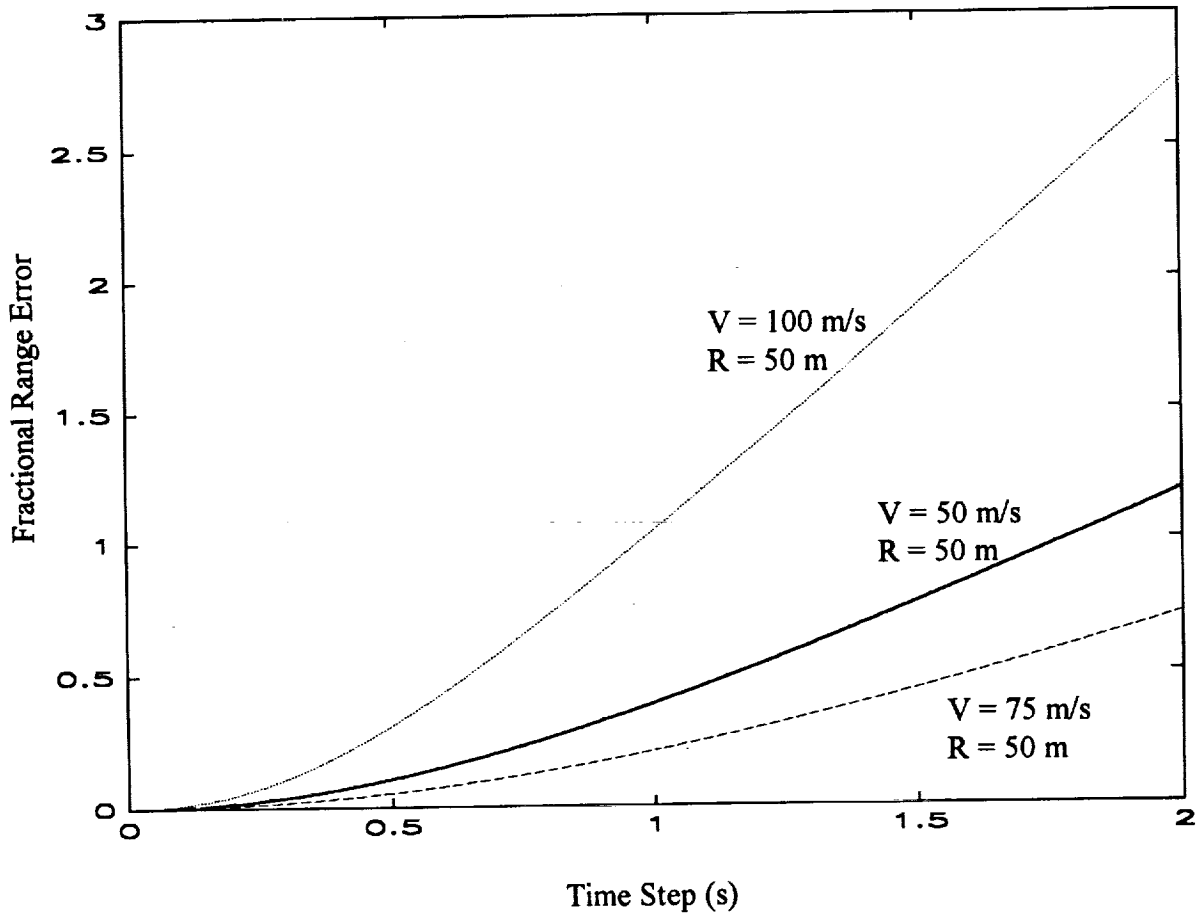
Figure 4. Fractional range error vs time step for various values of V and R.

peaks which are spaced nearby in frequency will overlap and interfere in the phase domain. It should be possible to obtain equations which will perform the CSD analysis for peaks containing multiple components, but it is necessary to know beforehand how many components are present. This may not be possible in a field application where any number of sources may pass the sensor.

The CSD method was tested on the simulated cases found in table 1. Error values (which can be found in table 2) were within expected limits of the values that were predicted in the graphs in figure 4. Further tests were performed using experimental data, and sources of this data are listed in table 3. The true values of position as a function of time were used to calculate velocity (actual values were obtained from radar telemetry). The predictions made by the CSD method and error values from these calculations can be found in table 4. Note that the error found in these tables is somewhat larger than predicted in figure 4. This is caused by the addition of background noise into the peaks that were used to calculate the accurate frequency.

The CSD allowed an accurate determination of the frequency from a small portion of the spectrum, but the deconvolution of multiple signals using this method had some limitations. The presence of multiple signals in a single peak is not accounted for in the derivation of this method. The condition of peaks that are overlapping or not fully resolved cause the phase information for a particular peak to be corrupted, thus severely complicating the deconvolution of the peak.

Successive Differences

Another way of extracting the frequency and velocity is to first perform an FFT on the entire sample of data (all the way through the approach and departure of the source). The results of the FFTs are shown in figures 5-9. The maxima on the ends of the u-shaped features in these figures are the frequency values of the source at the incoming and outgoing frequencies. It is possible to derive an analytic expression for the u-shaped features in the ideal case.

The problem of extracting frequency as a function of time was addressed using the method of successive differences. The frequency resolution limit from equation 5 was overcome by computing the FFT of two intervals with sufficient length to produce the desired resolution. The successive intervals for each FFT had starting points separated by the desired time step. The differences between these two spectra were computed, and the remaining positive portion of the difference contains the peak values of the frequencies that were added into the signal during that time interval.

Table 1. Simulated helicopter acoustic data.

Runs Generated

Name of Run	Fundamental Frequency (Hz)	Length of Run (Sec)	CPA (m)	Speed (m/s)
Hela.dat	16	32	10	50
Helb.dat	16	32	50	50
Helc.dat	16	32	200	50
Held.dat	16	32	500	50
Hele.dat	16	32	10	100
Helf.dat	16	32	50	100
Helg.dat	16	32	200	100
Helh.dat	16	32	500	100
Heli.dat	16	32	10	250
Helj.dat	16	32	50	250
Helk.dat	16	32	200	250
Hell.dat	16	32	500	250

Table 2. Results of CSD analysis on multiple simulated single source signals.

Actual Fundamental Frequency (Hz)	Calculated Fundamental Frequency (Hz)	% Error	Actual CPA (m)	Calculated CPA (m)	% Error	Actual Speed (m/s)	Calculated Speed (m/s)	% Error
16	16.002	0.0125	10	19.87	98.7	50	49.99	0.02
16	16.004	0.025	50	60.57	21.1	50	49.91	0.18
16	16.017	0.10625	200	219.66	9.83	50	48.51	2.98
16	16.047	0.29375	500	399.52	20.1	50	41.87	16.26
16	15.998	0.0125	10	36.20	262	100	99.94	0.06
16	16.000	0	50	77.16	54.3	100	99.92	0.08
16	16.020	0.125	200	278.81	39.4	100	99.23	0.77
16	16.094	0.5875	500	634.80	26.9	100	95.09	4.91
16	16.003	0.01875	10	108.34	983.4	250	249.99	0.01
16	16.013	0.08125	50	124.01	149.0	250	249.93	0.03
16	16.001	0.00625	200	768.65	284.3	250	249.92	0.03
16	16.003	0.01875	500	108.34	78.3	250	249.09	0.36
100	100	0	10	0	100	50	49.99	0.02
100	100.008	0.008	50	59.41	18.82	50	49.9	0.20
100	100.101	0.101	200	219.79	9.895	50	48.4	3.20
100	100.289	0.289	500	401.97	19.606	50	41.97	16.1
100	100.002	0.002	10	34.32	243.2	100	99.99	0.01
100	100.007	0.007	50	81.75	63.5	100	99.96	0.04
100	100.125	0.125	200	275.08	37.54	100	99.23	0.77
100	100.566	0.566	500	649.11	29.822	100	95.54	4.463

Table 3. Experimental helicopter acoustic data.
From the JAPE, run indicates JAPE run number in WES database.

Case	Run
Case A	WSR147a
Case B	WSR148a
Case C	WSR149a
Case D	WSR150a
Case E	WSR151a
Case F	WSR152a
Case G	WSR156a
Case H	WSR157a

Table 4. Results of CSD analysis on experimental data.

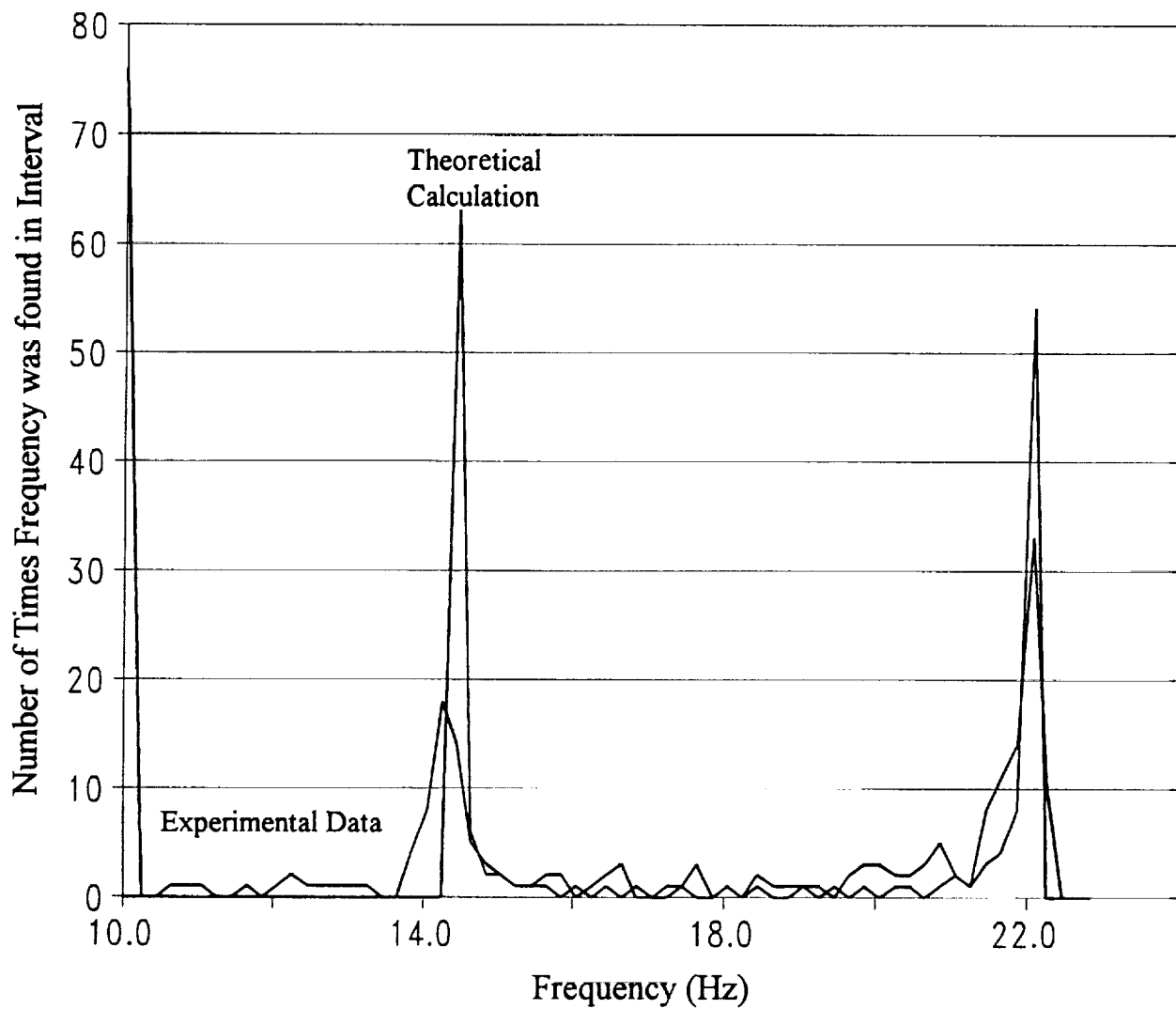| Case	Radar Velocity	CSD Velocity	Percent Error Velocity	Radar Range	CSD Range	Percent Error Range
A	51.4	56.7	10.3	51.0	41.0	19.6
B	52.0	56.4	8.4	105.4	54.0	48.8
C	54.2	56.3	4.0	105.2	42.0	60.1
D	73.8	71.7	2.8	108.7	99.0	8.9
E	70.9	69.4	2.1	98.2	54.0	45.0
F	75.0	75.2	0.3	109.3	62.0	43.3
G	47.1	57.1	21.1	206.4	141.0	31.7
H	44.8	49.6	10.7	320.5	187.0	41.7

Figure 5. Histogram of frequency from approach through departure.
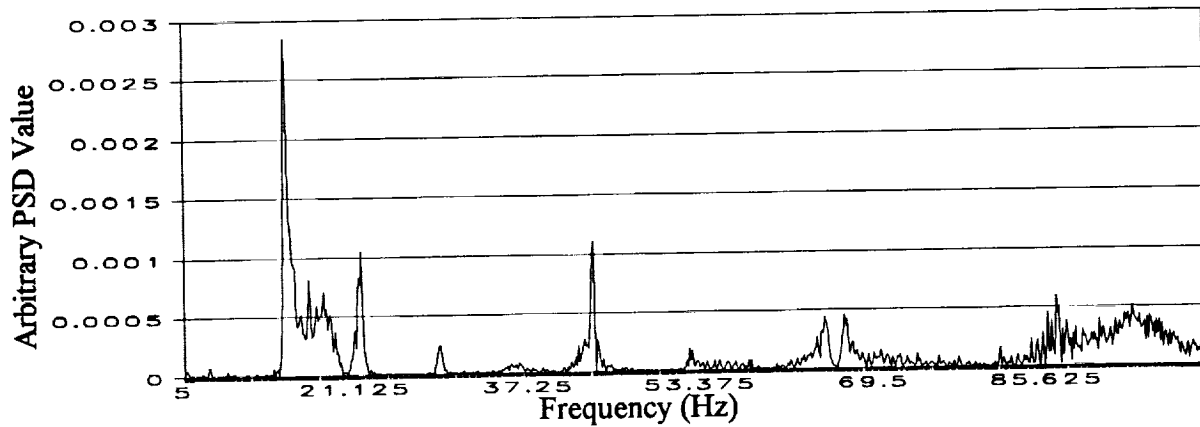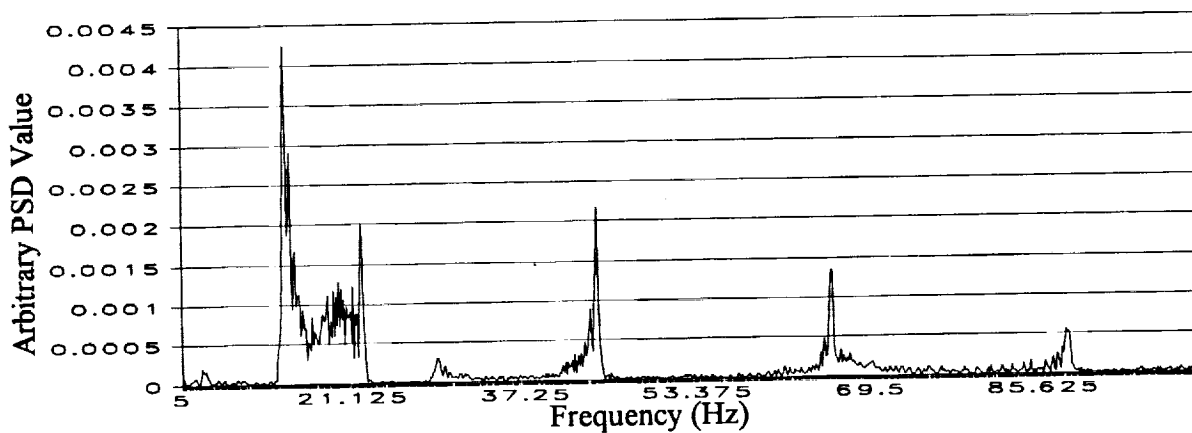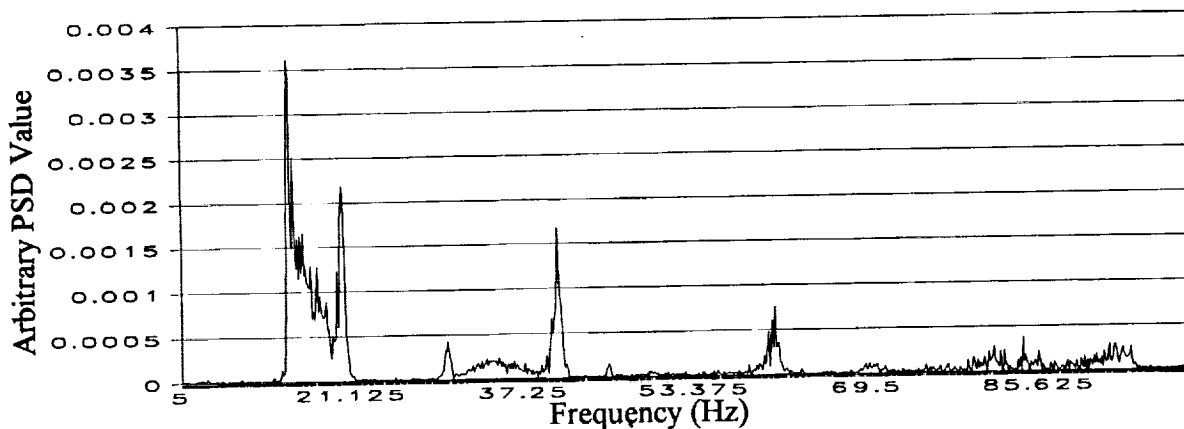
Figure 6. Selected PSD plots for 30 second extractions of time traces about CPA.
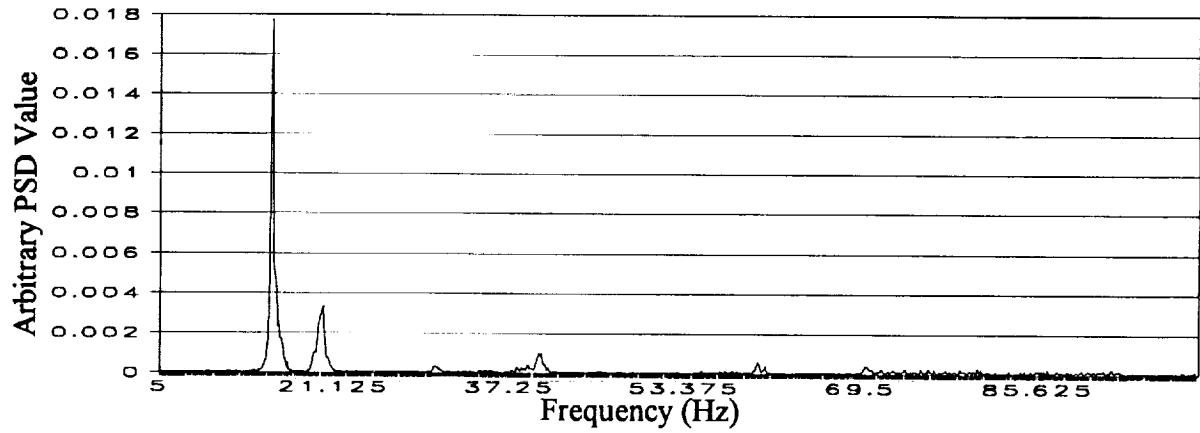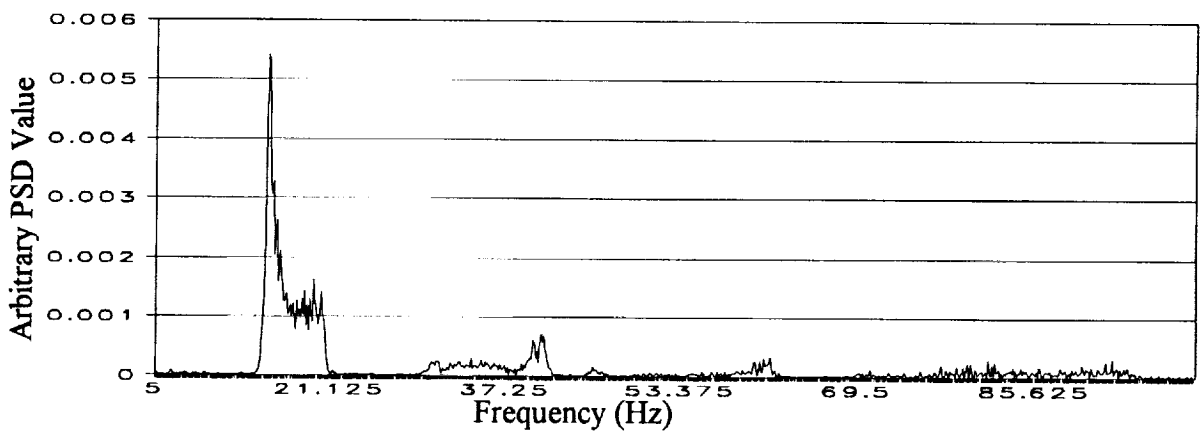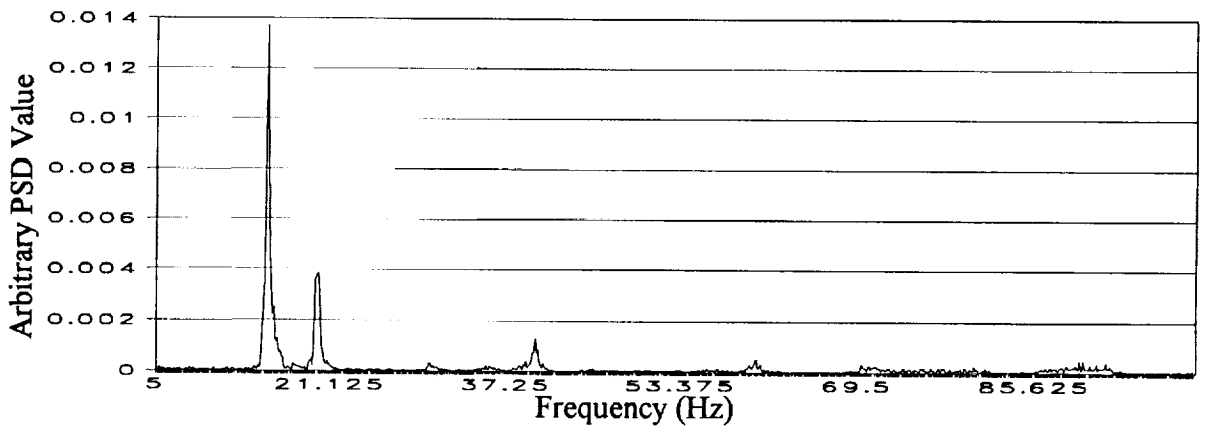
Figure 7. Selected PSD plots for 15 second extractions of time traces about CPA.
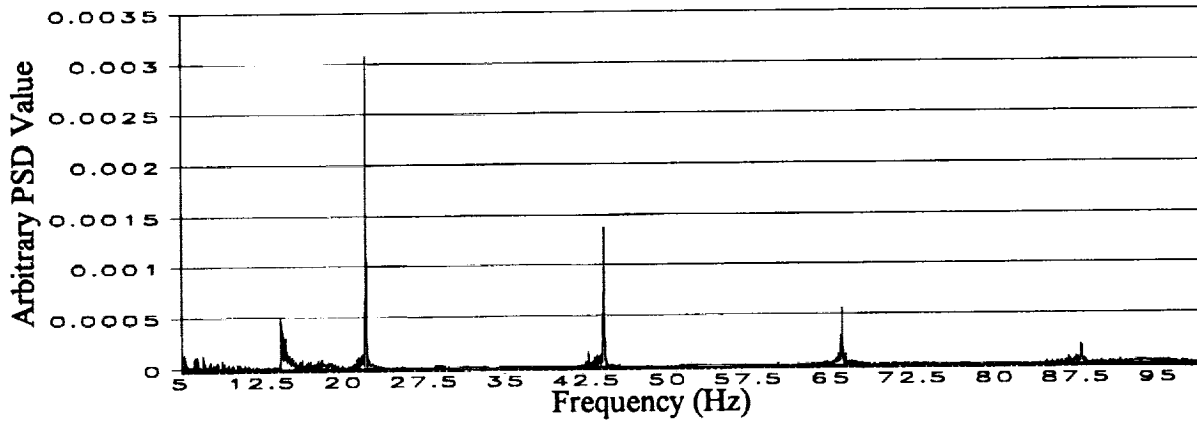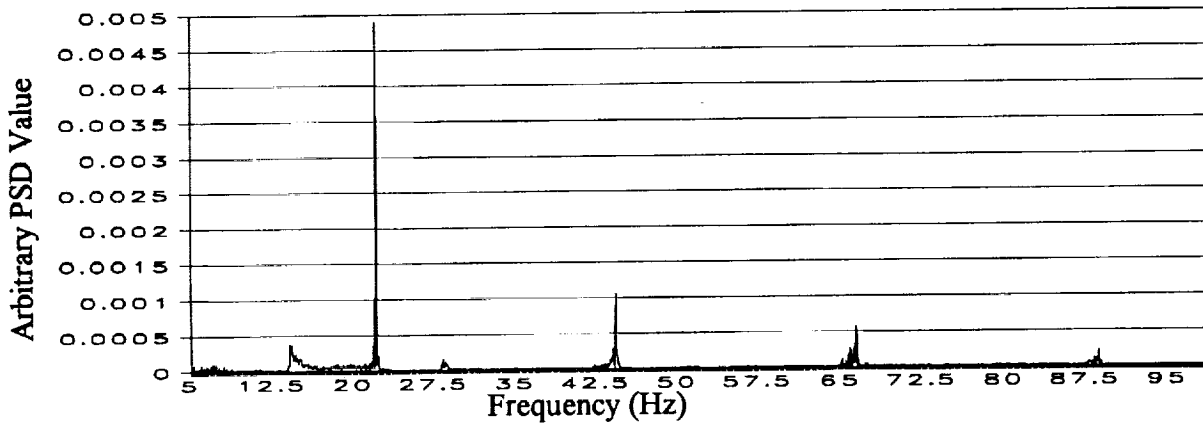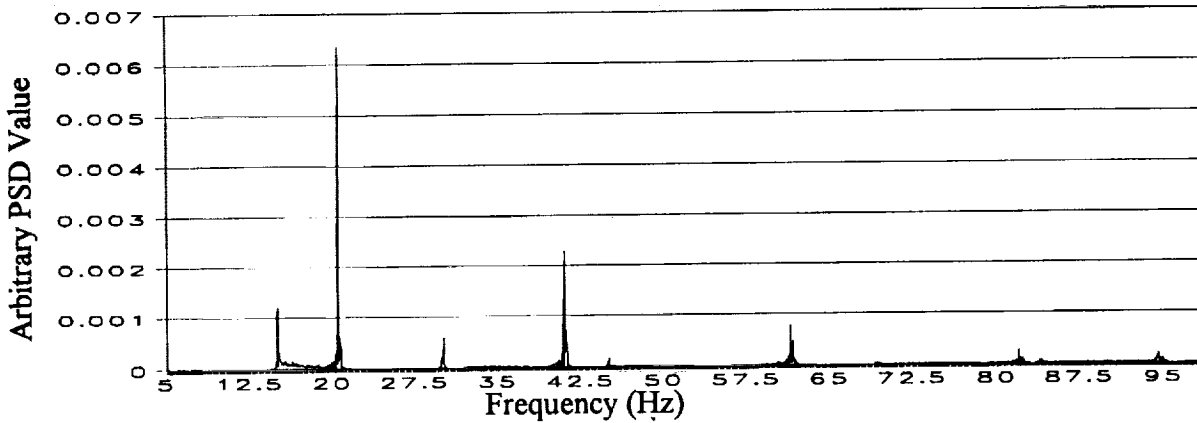
Figure 8. Selected PSD plots for 15 second extractions of time traces about CPA.
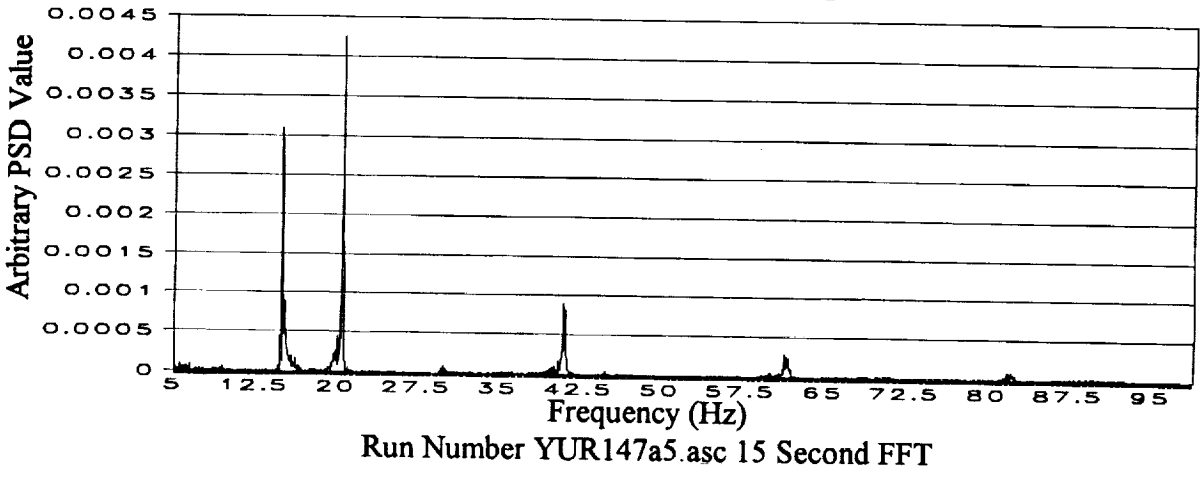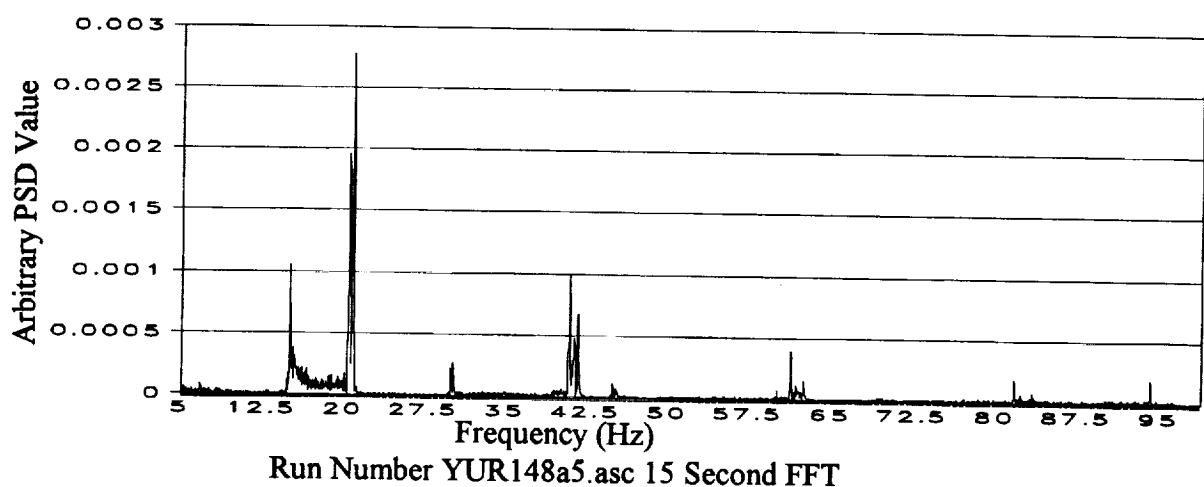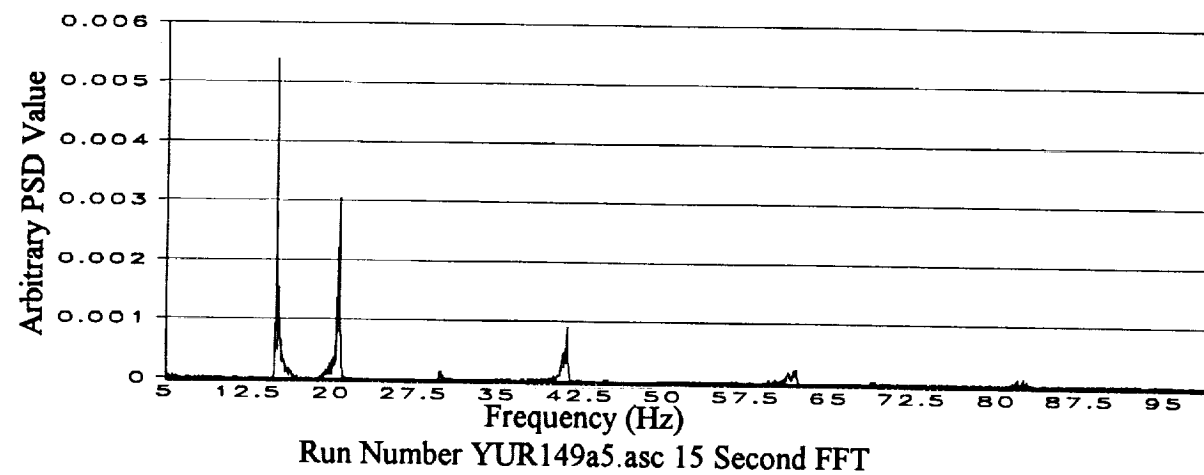
Figure 9. Selected PSD plots for 15 second extractions of time traces about CPA.

The method of successive differences exploits the fact that as the period in the sample to be transformed is increased, the resolution of the result will also increase. This method was adapted from a commonly accepted practice in nuclear spectroscopy. In determining the half-life of short-lived isotopes in nuclear physics, it is a common practice to acquire a spectrum and save it, then continue to acquire into that spectrum for some time. The difference between the two spectra will contain the amount of decays that occurred for each peak during that time, and a half-life calculation can easily be made. Similarly, the differences between two amplitude normalized high resolution FFTs will represent the changes that occurred during the period between the acquisition of the two time traces.

By first determining the incoming and outgoing frequencies, the stationary fundamental frequency of the source was calculated. From this information the time trace was then searched at a high resolution in order to determine the slope of the frequency versus time function as the fundamental peak passes through the stationary value. This process was automated along with peak search algorithms to identify peaks and extract frequency information from them. The values of range, velocity, and frequency were the output of this code. Errors in output from this method agree with what is expected from the theoretical limits.

Data processed with the CSD method was analyzed using this method. The results of the simulated and experimental runs, mentioned previously in tables 1 and 3, are presented in tables 5 and 6.

Comparison of Methods

While both methods produced results which agree with the theoretical analysis of the error in the ideal case, the SD method had an advantage over the CSD when there are multiple signals in a peak. In addition to the multiple peak problem, the CSD displayed a loss of accuracy when dealing with sections of time trace that had a duration of less than 0.25 second, but the SD has no such limit. It can be seen from figure 4, (which is a plot of error as a function of time step) that this 0.25 second limit gives an error as great as 15 percent for some cases. The disadvantage of the SD method is the intensive calculations which must be performed. The SD algorithm, written in the C programming language and executed on a 80486 class 33 MHz personal computer, took approximately twice the time to process a section that would be required for it to run in a real time mode, however this code was not optimized.

150

Table 5. Results of SD analysis on multiple simulated single source signals

Actual Fundamental Frequency (Hz)	Calculated Fundamental Frequency (Hz)	% Error	Actual CPA (m)	Calculated CPA (m)	% Error	Actual Speed (m/s)	Calculated Speed (m/s)	% Error
16.00	16.03	0.19	50.00	49.75	0.50	10.00	22.00	120.00
16.00	16.03	0.16	50.00	47.88	4.25	50.00	40.00	20.00
16.00	16.02	0.12	50.00	40.90	18.21	200.00	99.00	50.50
16.00	16.19	1.19	50.00	25.68	48.65	500.00	64.00	87.20
16.00	15.98	0.10	100.00	100.02	0.02	10.00	48.00	380.00
16.00	16.02	0.12	100.00	98.79	1.21	50.00	68.00	36.00
16.00	16.16	1.00	100.00	93.88	6.12	200.00	117.00	41.50
16.00	16.26	1.60	100.00	79.83	20.17	500.00	194.00	61.20
16.00	15.99	0.05	250.00	250.03	0.01	10.00	122.00	1120.00
16.00	15.99	0.05	250.00	250.03	0.01	50.00	124.00	148.00
16.00	16.17	1.08	250.00	248.68	0.53	200.00	240.00	20.00
16.00	16.61	3.79	250.00	245.00	2.00	500.00	441.00	11.80

Table 6. Results of SD analysis on experimental data.

Case	Radar Velocity	CSD Velocity	Percent Error Velocity	Radar Range	CSD Range	Percent Error Range
A	51.4	55.8	8.5	51.0	45.8	10.2
B	52.0	53.8	3.4	105.4	69.7	33.9
C	54.2	52.4	3.2	105.2	72.6	31.0
D	73.8	72.9	1.2	108.7	99.0	8.9
E	70.9	71.1	0.3	98.2	78.3	20.3
F	75.0	74.8	0.3	109.3	92.4	15.5
G	47.1	52.1	10.5	206.4	141.0	31.7
H	44.8	47.8	6.7	320.5	243.5	24.0

Both the CSD and SD methods were used with the equations from the previous study to calculate range, speed, and frequency information for a single source with some limited success. The problem of deconvoluting the signal was not solved at this time, but the key to developing a system for obtaining range information from multiple sources is to identify the number of sources present, and to track the signature peaks through their stationary frequencies.

Refinement of PAR through Artificial Neural Networks

The artificial neural network (ANN) is a computer algorithm that is modeled after the synapses and neurons in the brain. Recent research into the applications of this technique has found great success in classification and prediction using non-linear data. Investigations have been made using the ANN in a wide variety of fields and applications (including classification of military targets and medical diagnosis). The studies show that an ANN has the capability to learn a non-linear pattern. Because of this fact a study was planned to evaluate the feasibility of using an ANN to classify the source and possibly to determine the source type, quantity, velocity and range.

Back Propagation Training of an ANN

An ANN is an interconnected array of neurons. The first level of neurons, called the input layer, is connected to inner hidden layers of neurons by synapses. The last hidden layer of neurons is also connected to the output layer by synapses. The neurons in the hidden layers are made up of weight values which are established by training. The ANN is trained to recognize patterns in the data by learning many examples. The standard method of training is by back propagation. A transfer function for each neuron determines the value each neuron will output. Many possible modifications can be made to optimize the internal parameters of an ANN.

ANN Training, Testing, and Development

An ANN application was designed for the helicopter scenario and it was trained to recognize patterns in the data by learning many examples. The standard method of back propagation was used for training in this case. The standard sigmoid transfer function, as well as an input, output, and a single hidden layer of neurons, was chosen for the architecture of this network for

this application. Since there were only single runs of Huey and Blackhawk helicopters (no multiple runs) in the JAPE, a method to synthesize signals from more than one source was developed. A simulation code (further discussed in Appendix A) was also used to create signals from a third source. Data from each source were used in training the ANN.

The first ANN was trained on three data sets (listed in table 7), which included a single simulated source, a single helicopter (run WS147 from the JAPE) and a dual source synthesized from these two runs. A total of 350 one second time windows of the time traces were extracted from these three data sets at random, and 50 of these were retained for testing of the ANN. An FFT was performed on each of the 350 time windows, and the results were truncated to limit the frequency content to a range of 5 to 85 Hz. These frequency values were used as the input layer for the ANN. The ANN was then trained on the FFT of each of the 300 time windows until the average error was minimized. After the training was complete, the 50 one second windows retained for testing were fed into the ANN as inputs. The ANN was able to classify the source accurately 100 percent of the time, as can be seen in table 8.

After this initial success nine data sets were prepared on single and combinations of sources as shown in table 9. A total of 550 time windows were selected from these data sets, and 50 of these were again retained for testing. Another ANN was trained on the FFT of each of the 500 time windows to determine if the ANN could classify multiple helicopters. The ANN was able to classify the sources accurately 90 percent of the time in any of the combinations, and the results of the testing are presented in table 10. Selected FFT's from the test cases are presented in figures 10 - 27.

DISCUSSION AND CONCLUSIONS

It is feasible to develop the PAR concept into an algorithm that can be part of an operational sensor system. However, the PAR has several limitations discovered in this study that must be addressed before using such an algorithm. In the previous study the PAR concept was described as operable on a single sensor, but the selection of the time step for developing the Doppler shift curve is critical, depending on the speed of the source and the distance from the sensor. Selection of the wrong time step could cause the curve to have only one or two points during the Doppler shift, severely distorting the slope calculation. Because of this limitation, it would be advisable to use the PAR concept on multiple sensors. An array is not required (i.e., to perform beamforming), and the PAR algorithm can be used independently on each sensor (which can be

separated by relatively large distances). The PAR concept can also be used on multiple sources, but the Doppler shift curves for each of the sources present in the signal must be identified. Because of the mode of determining the range and velocity used by the PAR, the portion of the signals produced by each source must be used to produce separate Doppler shift curves for each source. The conventional methods of signal processing tested herein were not sufficient to produce the curves reliably for each source. Another limitation of the PAR concept is that the source has to pass through CPA and into the far-field before the calculation can be completed unless there is a priori knowledge of the stationary frequency of the source.

The use of an ANN to identify the sources and separate their signal contributions is feasible. However, only a limited test of the ANN for this purpose was performed in this study. It should be noted here that the 90 percent accuracy resulting from the ANN was probably not a major problem for application to the PAR concept. The ANN was not optimized, and was only trained with 500 examples. Training on additional samples would increase the accuracy of the ANN. The accuracy of the ANN classification was also affected by the distance from the sensor, because of degradation of the signal as it propagated through the atmosphere. The time windows were selected for distances up to 1.5 km from CPA, and the Doppler shift occurs within a few hundred meters of CPA. Therefore, the accuracy of the ANN classifier is higher in the area required for the analysis for the PAR concept. The use of an ANN could also be used to improve the response time of the PAR concept. Because of the capability of an ANN to identify the source, the calculation could be performed within a very short time of the source passing CPA.

RECOMMENDATIONS

The PAR concept has definite utility in the acoustic detection field, but because of the limitations discussed in this report, caution must be used in planning the deployment of a system with a PAR algorithm. A PAR algorithm might be more useful to supplement other acoustic detection algorithms (such as beamformers used in triangulation, etc.). The application of an ANN to the PAR concept using multiple sensors appears to have the necessary processing capability to overcome the limitations. The ability to classify and separate the sources in the measured signal allows the PAR algorithm to determine the stationary frequency and calculate the range and velocity of each source. These calculations can also be done as the source passes through CPA. A sequence of ANNs could also possibly be used to perform several portions of the signal processing required for the PAR concept. Further study of the PAR concept and the applicable ANN processing is recommended.

154

REFERENCE

[1] Olson, R.E., Cress, D.H. (1992). "Passive Acoustic Range Estimation of Helicopters," T.R. EL-92-13, U.S.A.E. Waterways Experiment Station, Vicksburg, Miss., 59 p.

Table 7. Index of cases used in first ANN training.

Case A	Simulated Source with 16 Hz Fundamental
Case B	WSR147a4 Blackhawk Helicopter from JAPE Data Set
Case C	Superposition of Cases A and B

Table 8. Results of ANN classification of first training case.

Case A		Case B		Case C		Results
Predicted	Actual	Predicted	Actual	Predicted	Actual	
0.00	0.00	0.00	0.00	0.99	1.00	Correct
1.00	1.00	0.00	0.00	0.00	0.00	Correct
1.00	1.00	0.00	0.00	0.00	0.00	Correct
1.00	1.00	0.00	0.00	0.03	0.00	Correct
0.00	0.00	1.00	1.00	0.00	0.00	Correct
0.00	0.00	1.00	1.00	0.00	0.00	Correct
0.00	0.00	1.00	1.00	0.00	0.00	Correct
0.00	0.00	1.00	1.00	0.00	0.00	Correct
1.00	1.00	0.00	0.00	0.00	0.00	Correct
0.00	0.00	1.00	1.00	0.00	0.00	Correct
0.99	1.00	0.01	0.00	0.00	0.00	Correct
0.00	0.00	1.00	1.00	0.00	0.00	Correct
0.00	0.00	0.00	0.00	1.00	1.00	Correct
0.00	0.00	1.00	1.00	0.00	0.00	Correct
1.00	1.00	0.00	0.00	0.00	0.00	Correct
1.00	1.00	0.00	0.00	0.00	0.00	Correct
0.00	0.00	1.00	1.00	0.00	0.00	Correct
0.00	0.00	0.02	0.00	1.00	1.00	Correct
0.00	0.00	0.00	0.00	1.00	1.00	Correct
0.00	0.00	1.00	1.00	0.00	0.00	Correct
0.01	0.00	0.00	0.00	1.00	1.00	Correct
1.00	1.00	0.00	0.00	0.00	0.00	Correct
0.00	0.00	1.00	1.00	0.00	0.00	Correct
0.00	0.00	0.08	0.00	0.99	1.00	Correct
0.00	0.00	0.00	0.00	1.00	1.00	Correct
0.98	1.00	0.06	0.00	0.01	0.00	Correct
1.00	1.00	0.00	0.00	0.00	0.00	Correct
0.81	1.00	0.01	0.00	0.00	0.00	Correct
0.00	0.00	0.00	0.00	1.00	1.00	Correct
1.00	1.00	0.00	0.00	0.00	0.00	Correct
0.00	0.00	0.00	0.00	1.00	1.00	Correct
0.00	0.00	0.00	0.00	1.00	1.00	Correct
0.00	0.00	0.00	0.00	1.00	1.00	Correct
1.00	1.00	0.00	0.00	0.00	0.00	Correct
0.00	0.00	0.00	0.00	1.00	1.00	Correct
1.00	1.00	0.04	0.00	0.00	0.00	Correct
0.00	0.00	0.00	0.00	1.00	1.00	Correct
1.00	1.00	0.00	0.00	0.00	0.00	Correct
0.97	1.00	0.18	0.00	0.00	0.00	Correct
0.00	0.00	1.00	1.00	0.00	0.00	Correct
1.00	1.00	0.00	0.00	0.00	0.00	Correct
1.00	1.00	0.00	0.00	0.00	0.00	Correct
0.00	0.00	0.00	0.00	1.00	1.00	Correct
1.00	1.00	0.00	0.00	0.00	0.00	Correct
0.98	1.00	0.16	0.00	0.00	0.00	Correct
0.00	0.00	0.00	0.00	1.00	1.00	Correct
0.00	0.00	1.00	1.00	0.00	0.00	Correct
0.00	0.00	0.00	0.00	1.00	1.00	Correct
0.00	0.00	0.00	0.00	1.00	1.00	Correct
0.00	0.00	0.02	0.00	1.00	1.00	Correct

Table 9. Index of cases used in second ANN training.

CASE	Description
Case A	Simulated Helicopter
Case B	Huey from Data Set WSMR010
Case C	Blackhawk from Data Set WS147
Case D	Two Summed Case A
Case E	Two Summed Case A and Case B
Case F	Two Summed Case A and Case C
Case G	Two Summed Case B
Case H	Two Summed Case B and Case C
Case I	Two Summed Case C

Table 10. Results of ANN classification of second training case.

	Case A	Case B	Case C	Case D	Case E	Case F	Case G	Case H	Case I	Results
actual	0.00	0.00	1.00	0.00	0.00	0.00	0.00	0.00	0.00	
predicted	0.00	0.00	1.00	0.00	0.00	0.00	0.00	0.00	0.00	Correct
actual	0.00	1.00	0.00	0.00	0.00	0.00	0.00	0.00	0.00	
predicted	0.00	1.00	0.00	0.00	0.00	0.00	0.00	0.00	0.00	Correct
actual	0.00	0.00	0.00	0.00	0.00	0.00	0.00	0.01	0.66	
predicted	0.00	0.00	0.00	0.00	0.00	0.00	0.00	0.00	1.00	Correct
actual	0.00	0.95	0.00	0.00	0.00	0.00	0.39	0.00	0.00	
predicted	0.00	1.00	0.00	0.00	0.00	0.00	0.00	0.00	0.00	Correct
actual	0.00	0.00	0.00	0.00	0.00	0.00	0.00	1.00	0.01	
predicted	0.00	0.00	0.00	0.00	0.00	0.00	0.00	1.00	0.00	Correct
actual	0.00	0.92	0.00	0.00	0.00	0.00	0.04	0.02	0.00	
predicted	0.00	1.00	0.00	0.00	0.00	0.00	0.00	0.00	0.00	Correct
actual	0.00	0.00	0.00	0.00	0.00	0.00	0.00	1.00	0.01	
predicted	0.00	0.00	0.00	0.00	0.00	0.00	0.00	1.00	0.00	Correct
actual	0.00	1.00	0.00	0.00	0.00	0.00	0.05	0.00	0.00	
predicted	0.00	1.00	0.00	0.00	0.00	0.00	0.00	0.00	0.00	Correct
actual	0.00	0.00	1.00	0.00	0.00	0.00	0.00	0.00	0.00	
predicted	0.00	0.00	1.00	0.00	0.00	0.00	0.00	0.00	0.00	Correct
actual	0.00	0.00	0.46	0.00	0.00	0.00	0.00	0.04	0.00	
predicted	0.00	0.00	1.00	0.00	0.00	0.00	0.00	0.00	0.00	Correct
actual	0.00	0.99	0.00	0.00	0.00	0.00	0.03	0.00	0.00	
predicted	0.00	1.00	0.00	0.00	0.00	0.00	0.00	0.00	0.00	Correct
actual	0.00	0.00	0.00	0.00	0.00	0.00	0.00	1.00	0.01	
predicted	0.00	0.00	0.00	0.00	0.00	0.00	0.00	1.00	0.00	Correct
actual	0.00	0.00	0.00	0.00	0.00	0.00	0.00	0.99	0.01	
predicted	0.00	0.00	0.00	0.00	0.00	0.00	0.00	1.00	0.00	Correct
actual	0.00	0.28	0.00	0.00	0.00	0.00	0.93	0.00	0.00	
predicted	0.00	1.00	0.00	0.00	0.00	0.00	0.00	0.00	0.00	Incorrect
actual	0.00	0.00	0.11	0.00	0.00	1.00	0.00	0.00	0.00	
predicted	0.00	0.00	0.00	0.00	0.00	1.00	0.00	0.00	0.00	Correct
actual	0.00	0.00	0.00	0.00	0.00	0.00	1.00	0.00	0.00	
predicted	0.00	0.00	0.00	0.00	0.00	0.00	1.00	0.00	0.00	Correct
actual	0.00	0.00	0.00	0.00	0.00	0.08	0.00	0.00	0.97	
predicted	0.00	0.00	0.00	0.00	0.00	0.00	0.00	0.00	1.00	Correct

158

Table 10. Results of ANN classification of second training case (continued)

	Case A	Case B	Case C	Case D	Case E	Case F	Case G	Case H	Case I	Results
actual	0.00	0.00	0.00	0.00	0.00	0.00	0.00	1.00	0.01	
predicted	0.00	0.00	0.00	0.00	0.00	0.00	0.00	1.00	0.00	Correct
actual	0.00	0.00	0.31	0.00	0.66	0.00	0.00	0.00	0.00	
predicted	0.00	0.00	1.00	0.00	0.00	0.00	0.00	0.00	0.00	Incorrect
actual	0.00	1.00	0.00	0.00	0.00	0.00	0.00	0.00	0.00	
predicted	0.00	1.00	0.00	0.00	0.00	0.00	0.00	0.00	0.00	Correct
actual	0.00	0.00	0.00	0.00	0.60	1.00	0.00	0.00	0.00	
predicted	0.00	0.00	0.00	0.00	1.00	0.00	0.00	0.00	0.00	Correct
actual	0.00	0.00	0.00	0.00	0.00	0.00	0.99	0.02	0.00	
predicted	0.00	0.00	0.00	0.00	0.00	0.00	1.00	0.00	0.00	Correct
actual	0.00	0.00	0.00	0.00	0.00	0.00	1.00	0.00	0.00	
predicted	0.00	0.00	0.00	0.00	0.00	0.00	1.00	0.00	0.00	Correct
actual	0.00	0.00	0.79	0.00	0.00	0.00	0.00	0.00	0.00	
predicted	0.00	0.00	1.00	0.00	0.00	0.00	0.00	0.00	0.00	Correct
actual	0.00	1.00	0.00	0.00	0.00	0.00	0.00	0.00	0.00	
predicted	0.00	1.00	0.00	0.00	0.00	0.00	0.00	0.00	0.00	Correct
actual	0.00	0.00	0.00	0.00	0.00	0.00	0.00	1.00	0.01	
predicted	0.00	0.00	0.00	0.00	0.00	0.00	0.00	1.00	0.00	Correct
actual	0.00	0.01	1.00	0.00	0.00	0.00	0.00	0.00	0.00	
predicted	0.00	0.00	1.00	0.00	0.00	0.00	0.00	0.00	0.00	Correct
actual	0.00	0.00	1.00	0.00	0.00	0.00	0.00	0.00	0.00	
predicted	0.00	0.00	1.00	0.00	0.00	0.00	0.00	0.00	0.00	Correct
actual	0.00	0.00	0.00	0.00	0.00	0.00	1.00	0.01	0.00	
predicted	0.00	0.00	0.00	0.00	0.00	0.00	1.00	0.00	0.00	Correct
actual	0.00	0.00	0.00	0.00	0.00	0.13	0.00	0.00	0.98	
predicted	0.00	0.00	0.00	0.00	0.00	0.00	0.00	0.00	1.00	Correct
actual	0.00	0.03	0.00	0.00	0.00	0.00	0.96	0.01	0.00	
predicted	0.00	1.00	0.00	0.00	0.00	0.00	0.00	0.00	0.00	Incorrect
actual	0.00	1.00	0.00	0.00	0.00	0.00	0.00	0.00	0.00	
predicted	0.00	1.00	0.00	0.00	0.00	0.00	0.00	0.00	0.00	Correct
actual	0.00	0.00	0.00	0.00	0.00	0.00	0.00	0.05	0.67	
predicted	0.00	0.00	0.00	0.00	0.00	0.00	0.00	0.00	1.00	Correct
actual	0.00	1.00	0.00	0.00	0.07	0.00	0.00	0.00	0.00	
predicted	0.00	1.00	0.00	0.00	0.00	0.00	0.00	0.00	0.00	Correct

Table 10. Results of ANN classification of second training case. (concluded)

|	Case A	Case B	Case C	Case D	Case E	Case F	Case G	Case H	Case I	Results
actual	0.00	0.00	0.00	0.00	1.00	0.00	0.00	0.00	0.00	
predicted	0.00	0.00	0.00	0.00	1.00	0.00	0.00	0.00	0.00	Correct
actual	0.00	1.00	0.00	0.00	0.00	0.00	0.00	0.00	0.00	
predicted	0.00	1.00	0.00	0.00	0.00	0.00	0.00	0.00	0.00	Correct
actual	0.00	1.00	0.00	0.00	0.00	0.00	0.00	0.00	0.00	
predicted	0.00	1.00	0.00	0.00	0.00	0.00	0.00	0.00	0.00	Correct
actual	0.00	1.00	0.00	0.00	0.00	0.00	0.00	0.00	0.00	
predicted	0.00	1.00	0.00	0.00	0.00	0.00	0.00	0.00	0.00	Correct
actual	0.00	0.00	0.00	0.00	0.00	0.00	0.00	1.00	0.01	
predicted	0.00	0.00	0.00	0.00	0.00	0.00	0.00	1.00	0.00	Correct
actual	0.00	1.00	0.00	0.00	0.00	0.00	0.00	0.00	0.00	
predicted	0.00	1.00	0.00	0.00	0.00	0.00	0.00	0.00	0.00	Correct
actual	0.00	0.00	0.00	0.00	0.00	0.00	0.00	0.88	0.07	
predicted	0.00	0.00	0.00	0.00	0.00	0.00	0.00	1.00	0.00	Correct
actual	0.00	0.00	1.00	0.00	0.00	0.00	0.00	0.00	0.00	
predicted	0.00	0.00	1.00	0.00	0.00	0.00	0.00	0.00	0.00	Correct
actual	0.00	0.99	0.48	0.00	0.00	0.00	0.00	0.00	0.00	
predicted	0.00	0.00	1.00	0.00	0.00	0.00	0.00	0.00	0.00	Incorrect
actual	0.00	0.00	0.00	0.00	0.00	0.00	0.00	0.09	0.64	
predicted	0.00	0.00	0.00	0.00	0.00	0.00	0.00	0.00	1.00	Correct
actual	0.00	0.00	0.98	0.00	0.00	0.00	0.00	0.00	0.00	
predicted	0.00	0.00	1.00	0.00	0.00	0.00	0.00	0.00	0.00	Correct
actual	0.00	1.00	0.00	0.00	0.00	0.00	0.00	0.00	0.00	
predicted	0.00	1.00	0.00	0.00	0.00	0.00	0.00	0.00	0.00	Correct
actual	0.00	0.00	0.00	0.00	0.00	0.00	0.00	0.99	0.01	
predicted	0.00	0.00	0.00	0.00	0.00	0.00	0.00	1.00	0.00	Correct
actual	0.00	0.00	0.00	0.00	0.00	0.00	0.00	0.99	0.01	
predicted	0.00	0.00	0.00	0.00	0.00	0.00	0.00	1.00	0.00	Correct
actual	0.00	0.00	0.67	0.00	0.00	0.00	0.00	0.01	0.00	
predicted	0.00	0.00	0.00	0.00	0.00	0.00	0.00	1.00	0.00	Incorrect
actual	0.00	0.00	0.00	0.00	0.00	0.00	1.00	0.00	0.00	
predicted	0.00	0.00	0.00	0.00	0.00	0.00	1.00	0.00	0.00	Correct
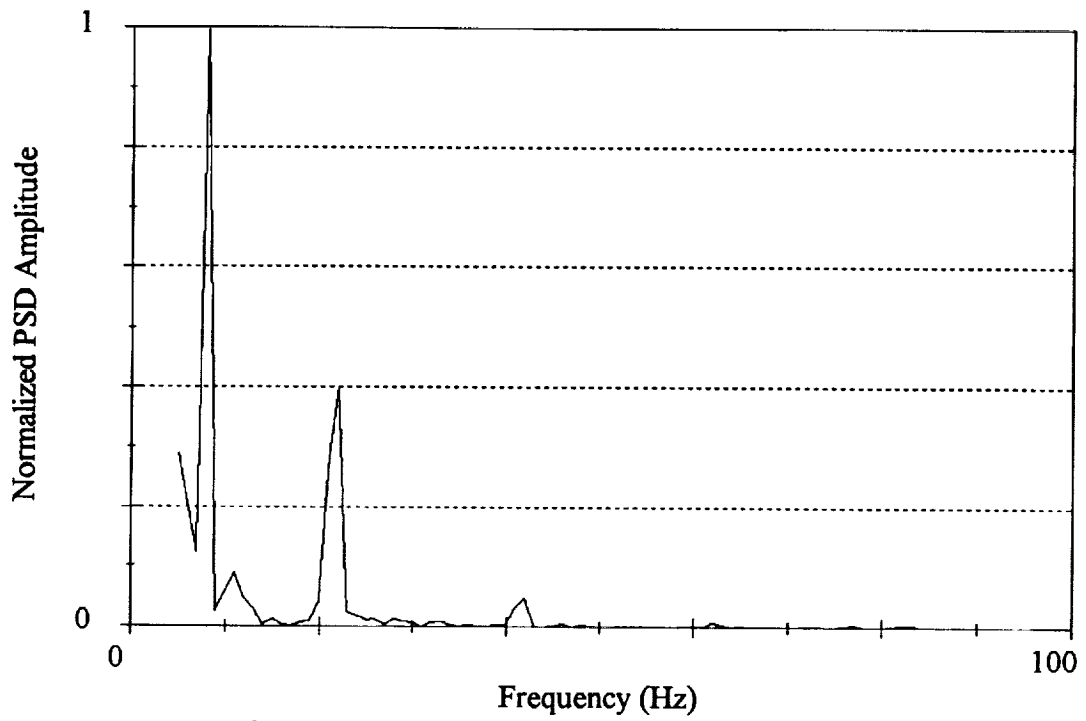
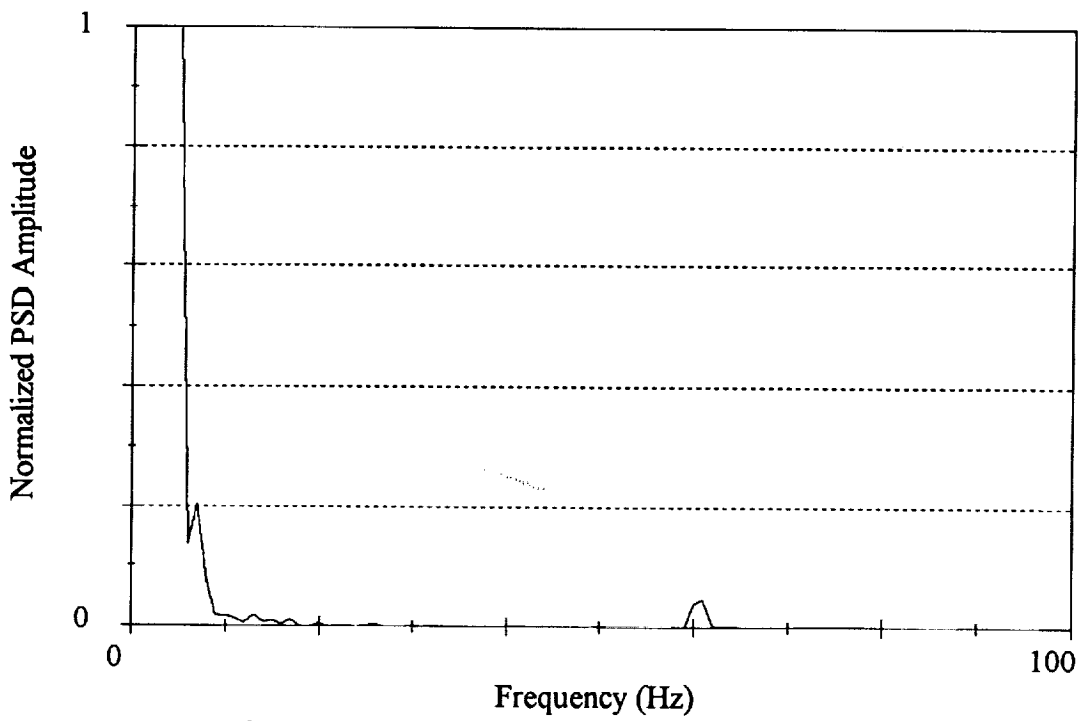Figure 10. PSD from case C used as sample number one.

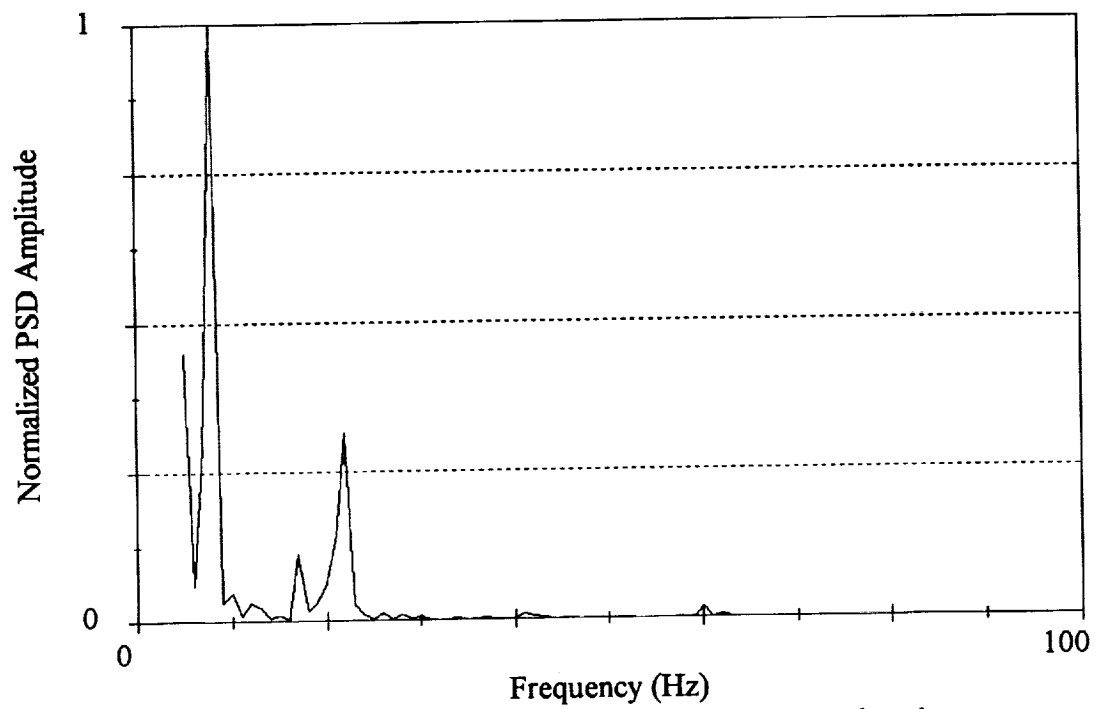Figure 11. PSD from case B used as sample number two.

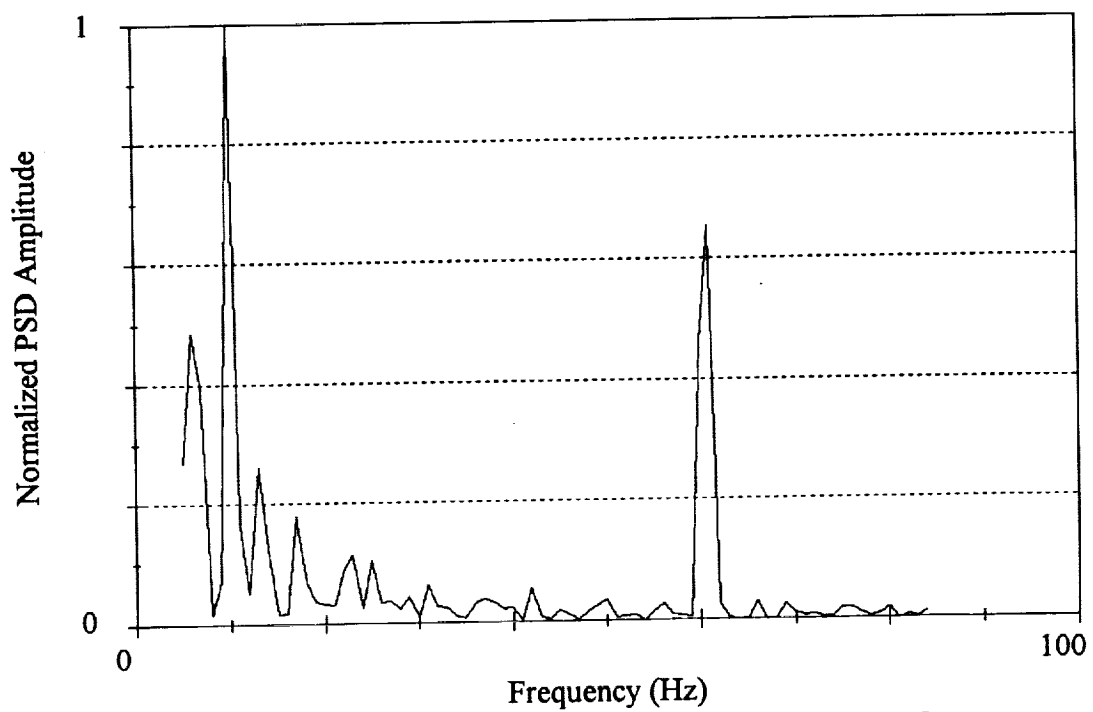Figure 12. PSD from case I used as sample number three.

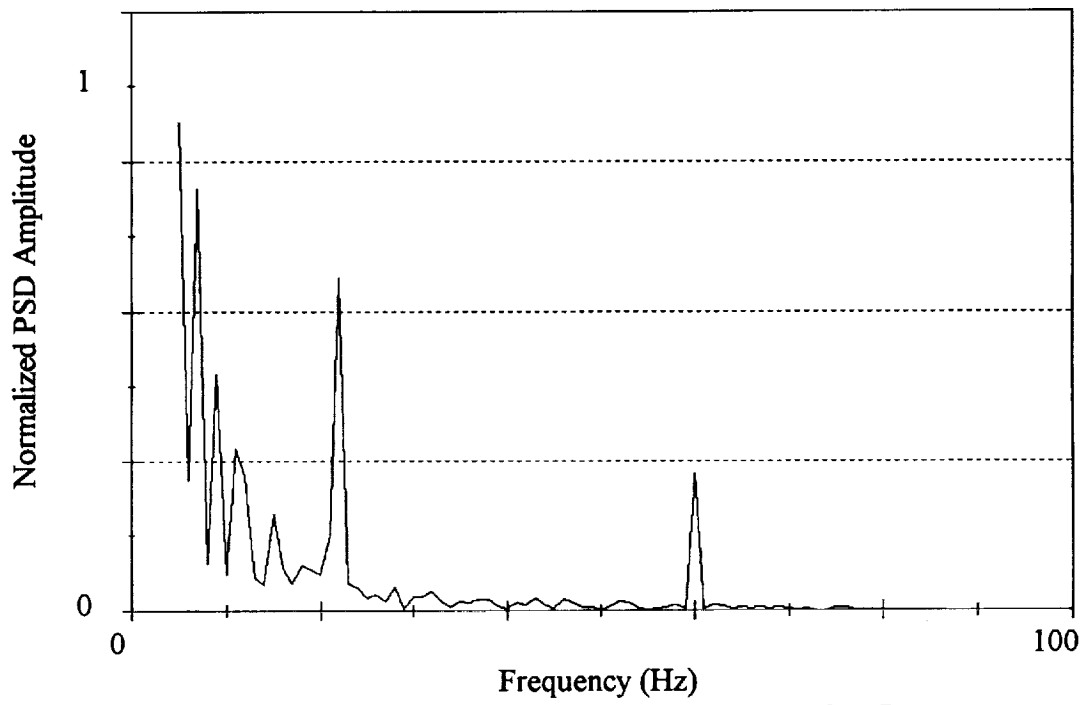Figure 13. PSD from case B used as sample number four.

162

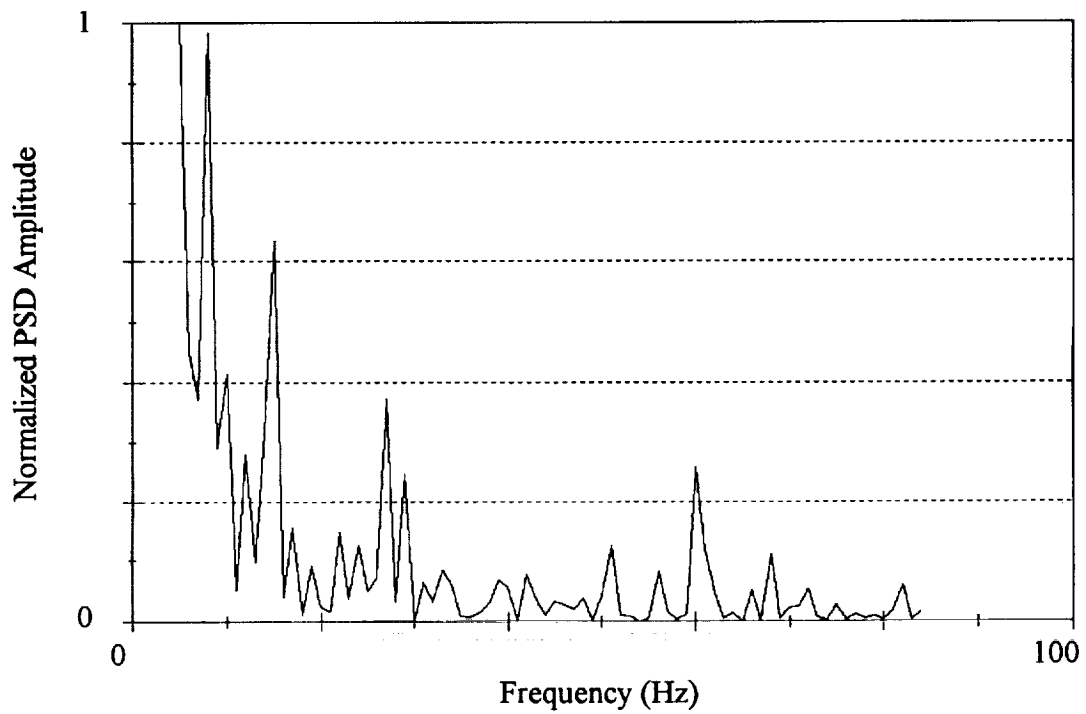Figure 14. PSD from case H in sample number five.
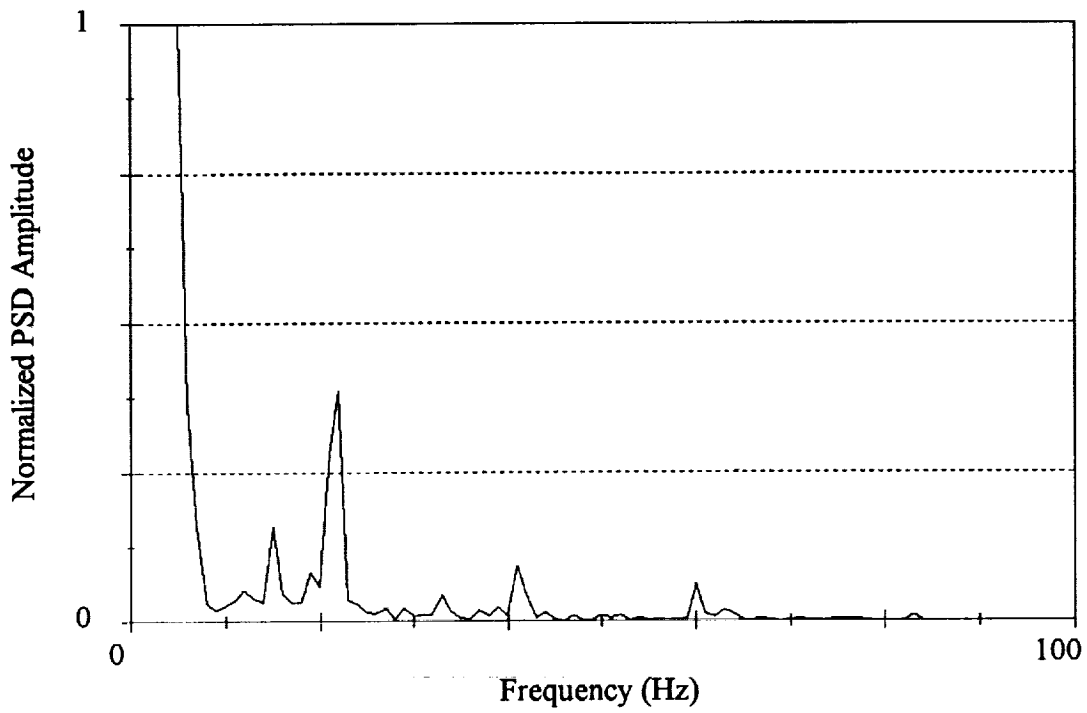

Figure 15. PSD from case B in sample number six.

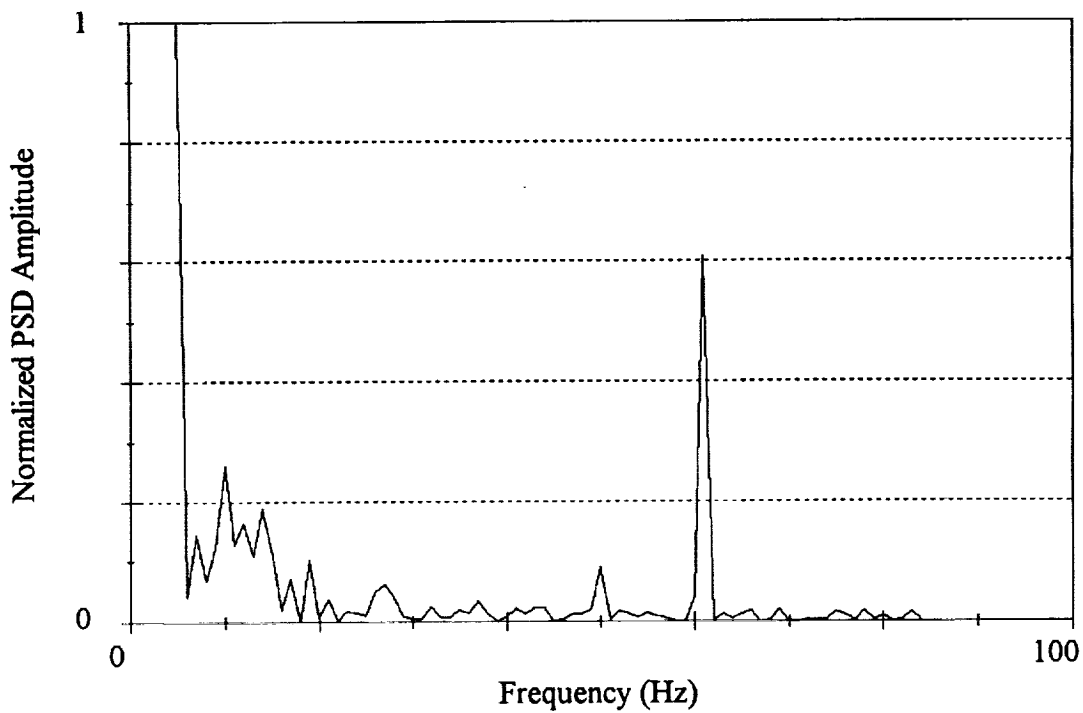Figure 16. PSD from case H in sample number seven.

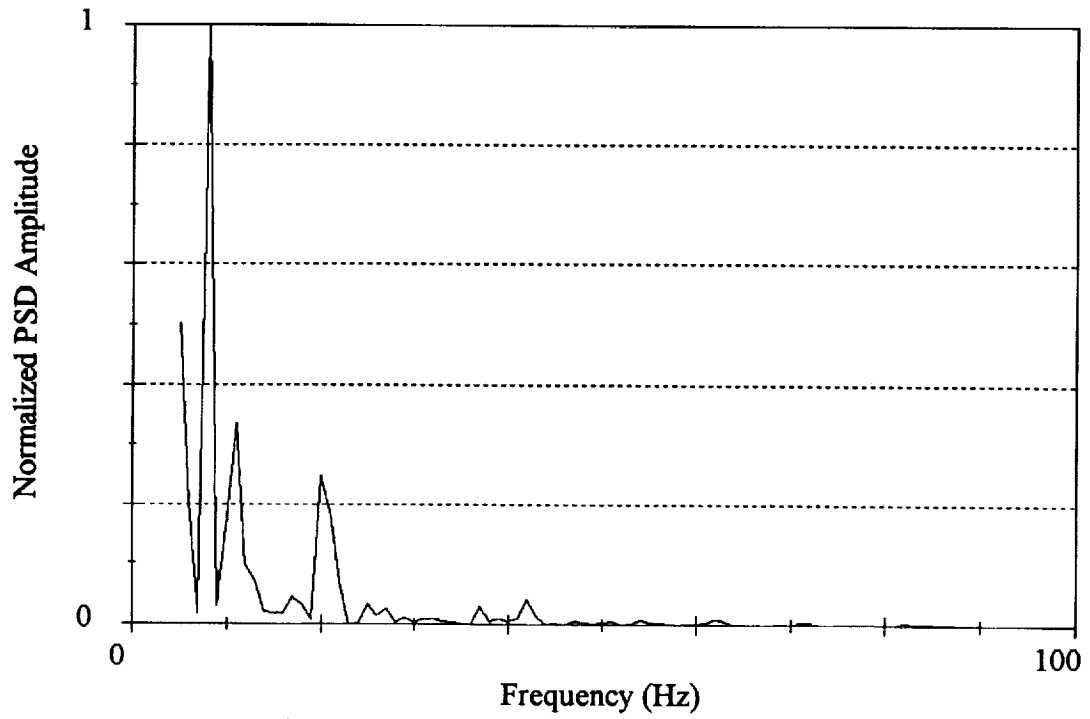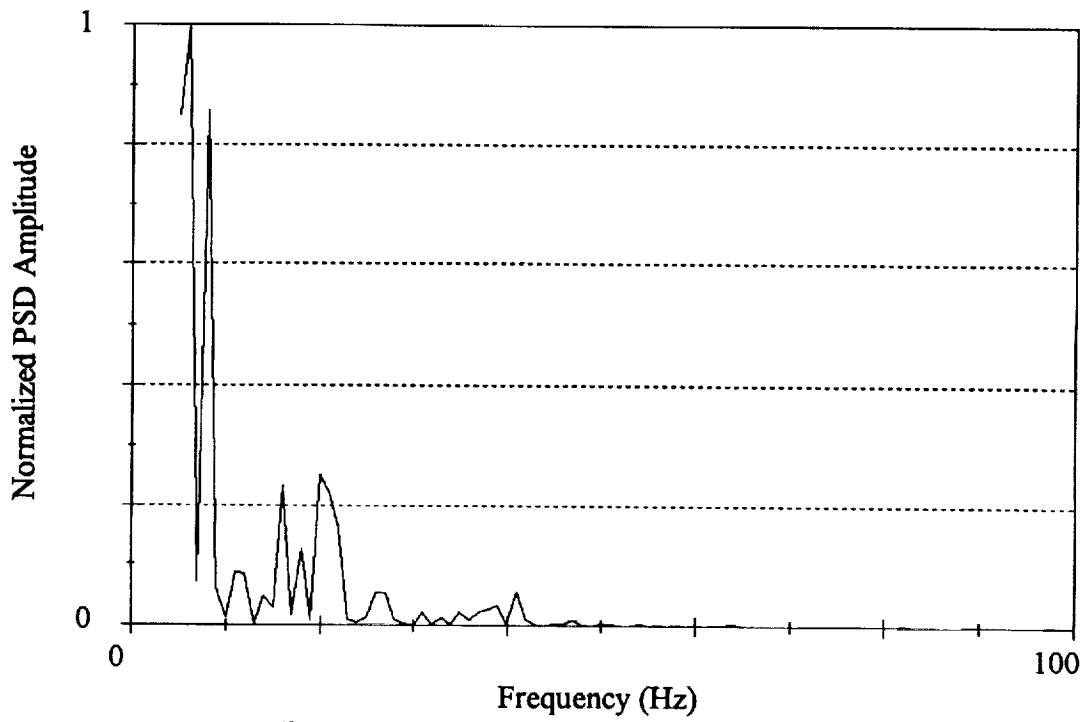Figure 17. PSD from case B in sample number eight.

Figure 18. PSD from case C in sample number nine.

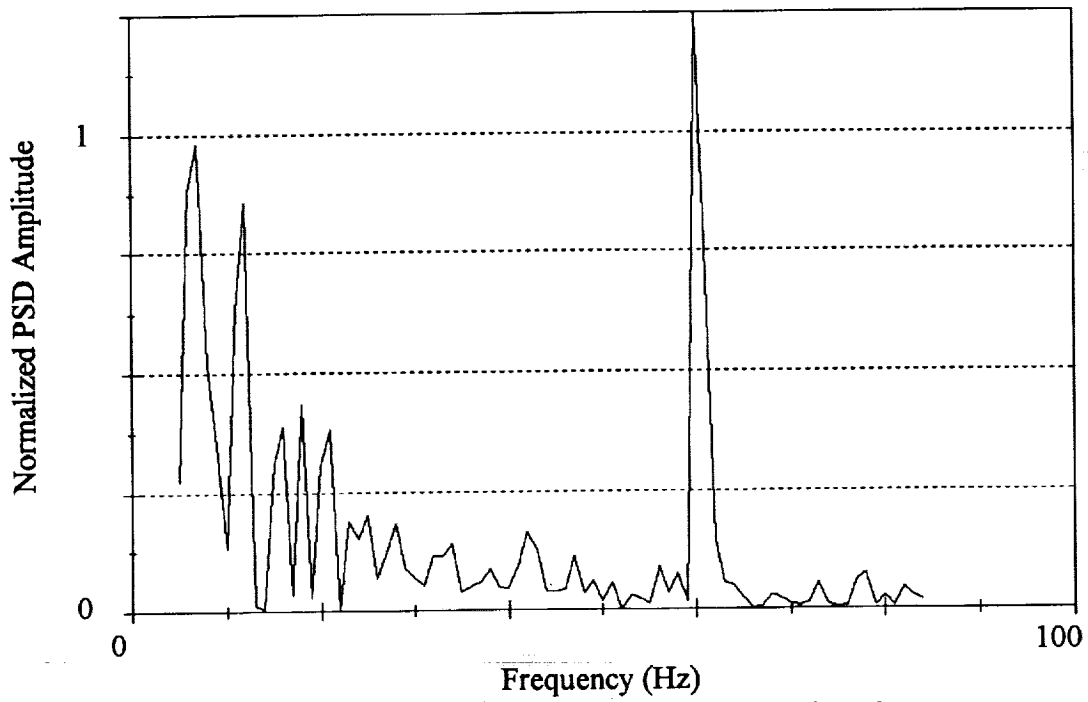Figure 19. PSD from case C in sample number ten.

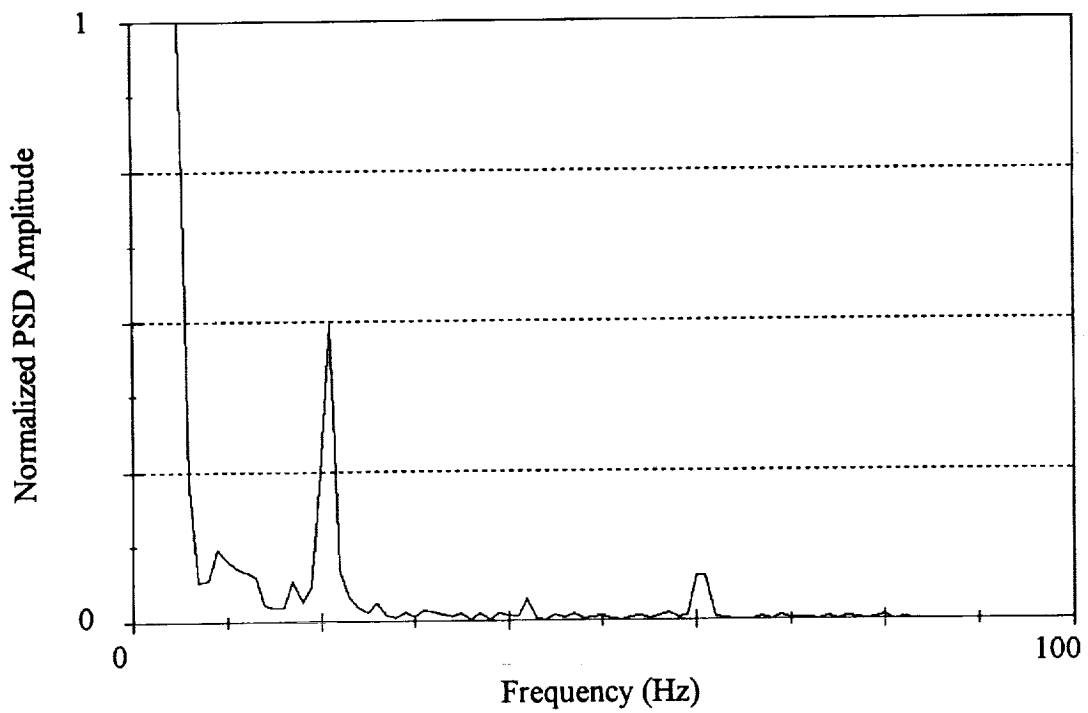Figure 20. PSD from case B in sample number eleven.

Figure 21. PSD from case H in sample number twelve.
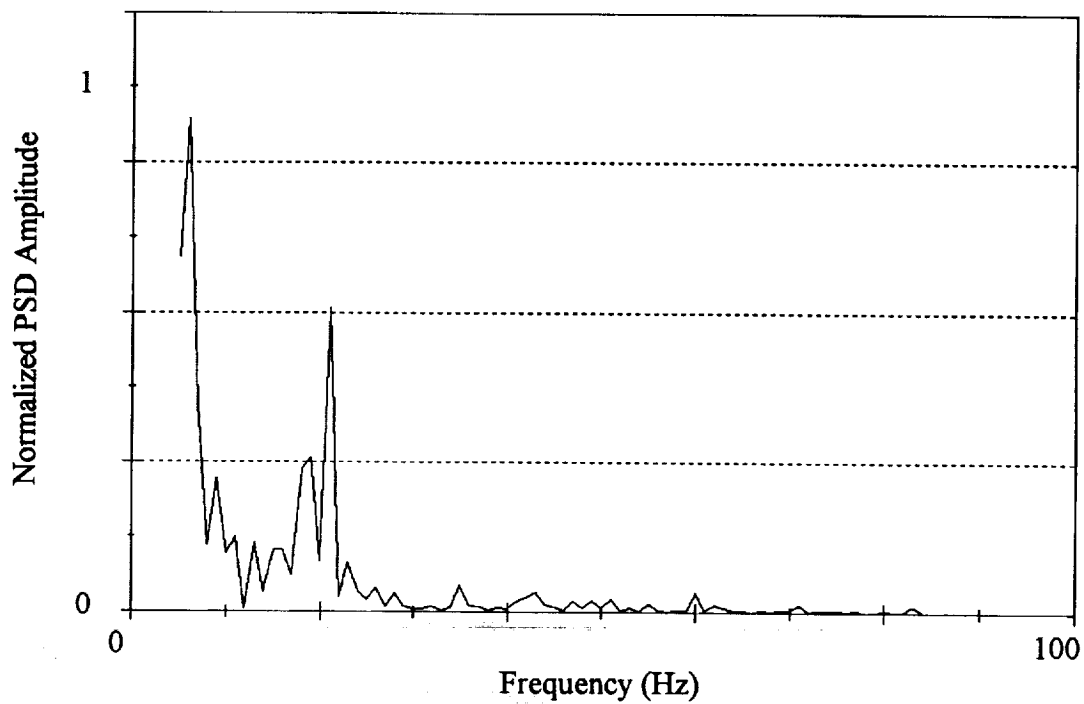
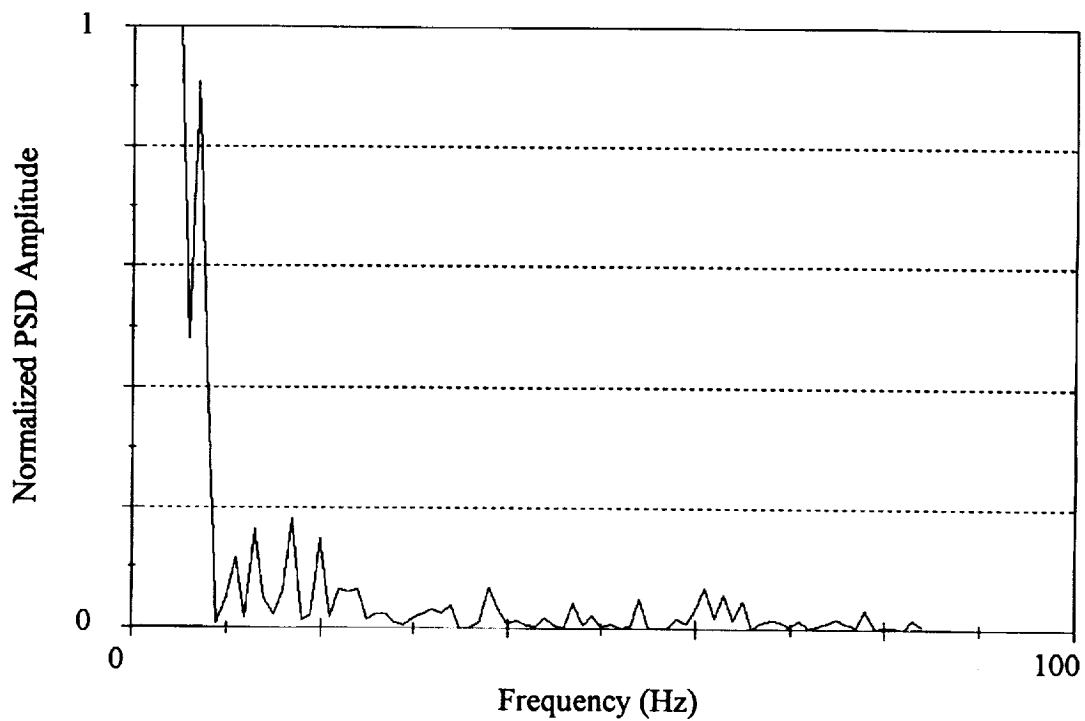Figure 22. PSD from case H in sample number thirteen.

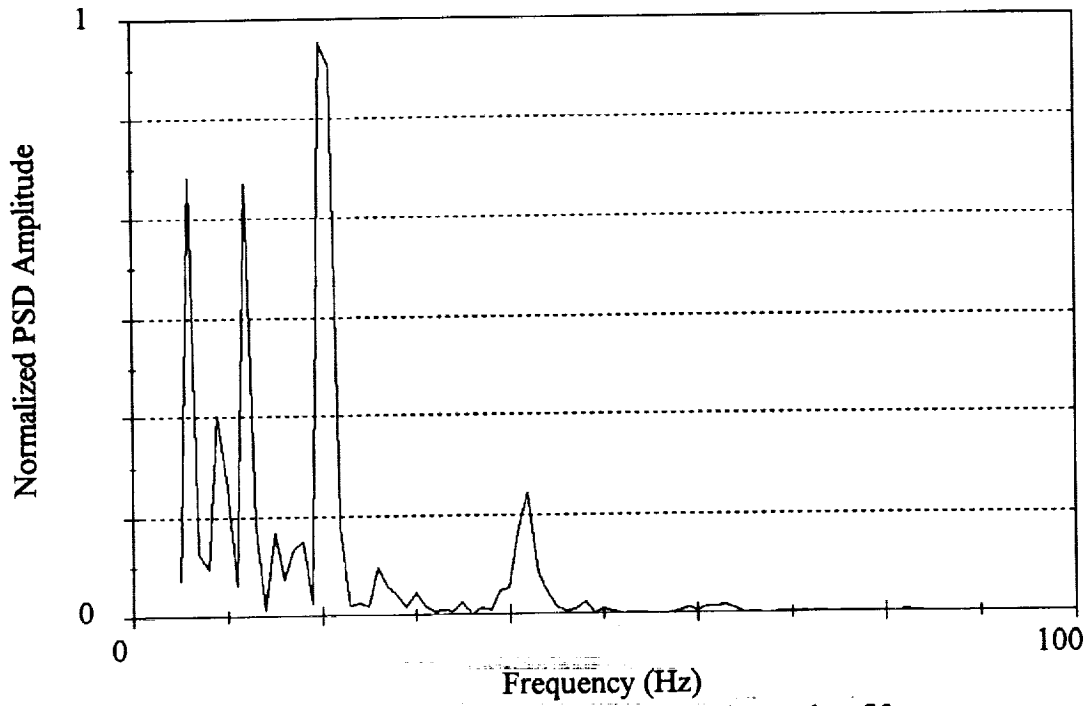Figure 23. PSD from case G in sample number fourteen.

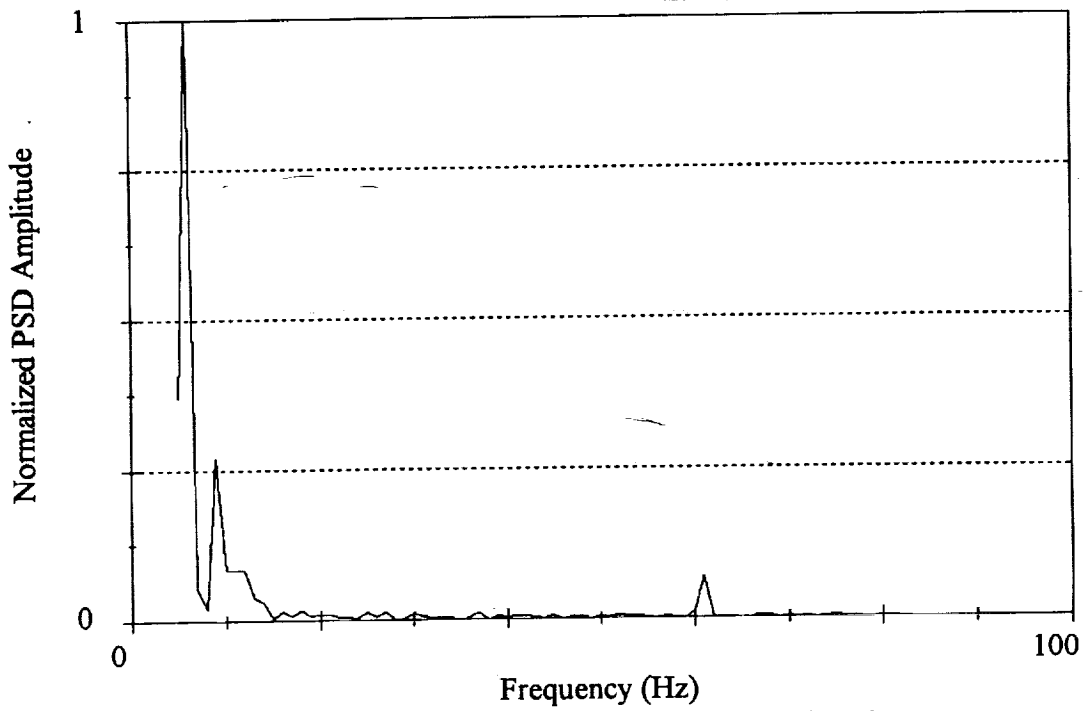Figure 24. PSD from case F in sample number fifteen.

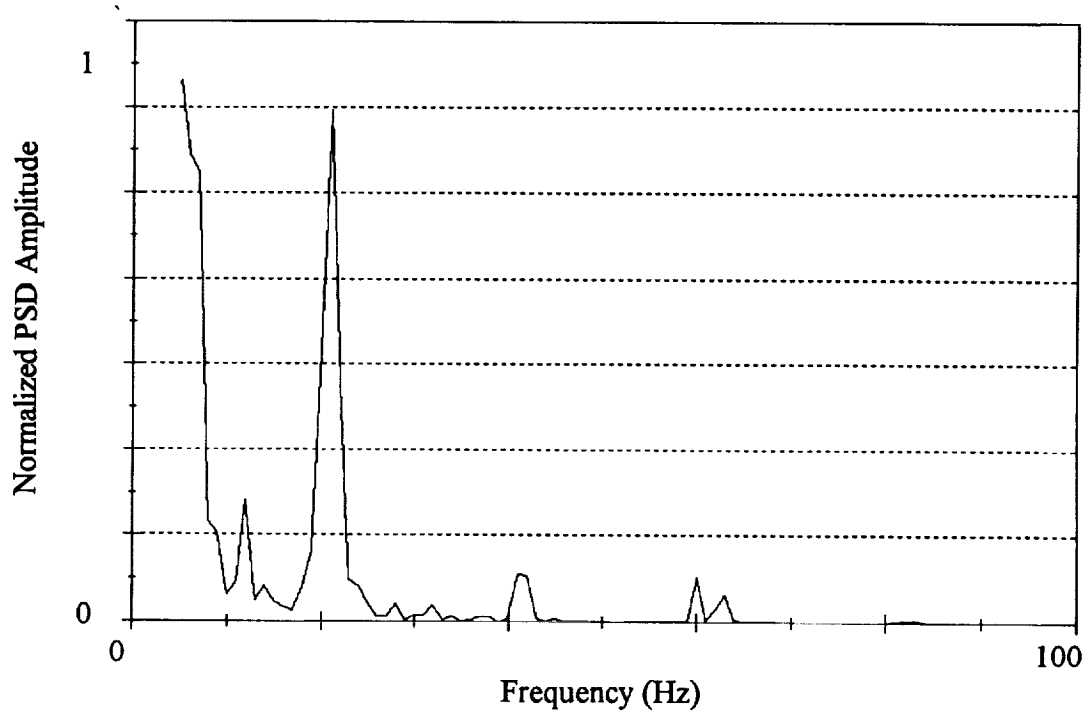Figure 25. PSD from case G in sample number sixteen.
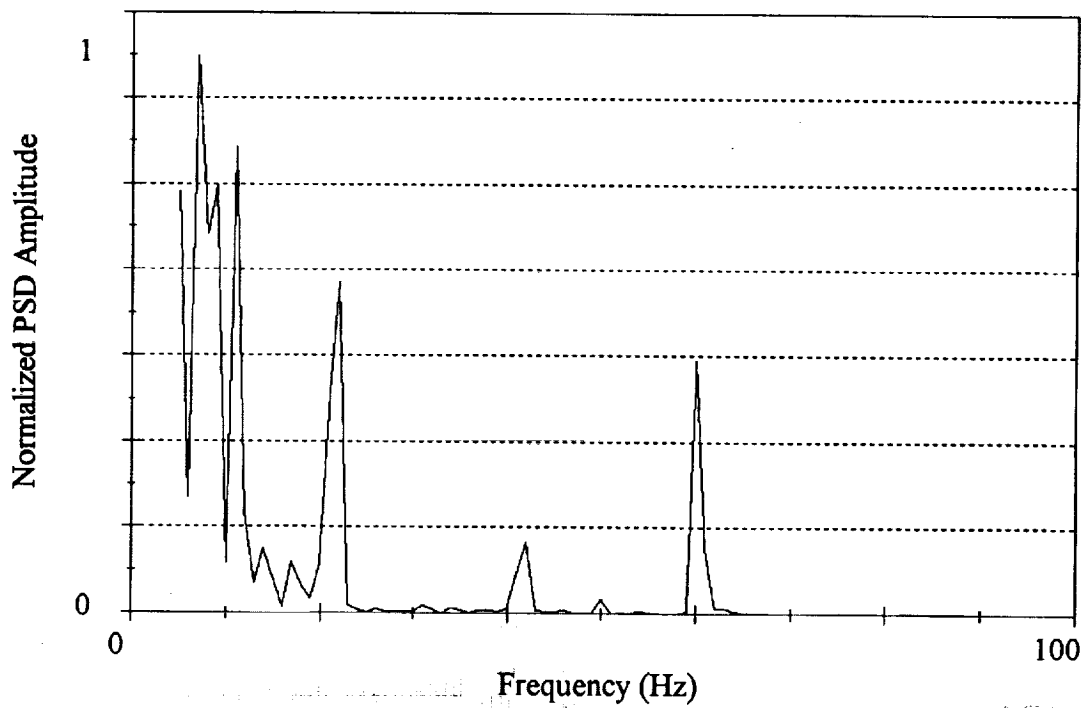
Figure 26. PSD from case I in sample number seventeen.

Figure 27. PSD from case H in sample number eighteen.

APPENDIX A SIMULATED SOURCES

In order to eliminate noise and effects that were associated with signals measured at field sites, and to provide any given case desired for testing, a computer code that would simulate a moving source was programmed. The code, which was written in Visual Basic, allowed the user to control the initial position, velocity, frequency, and phase of up to three sources, in addition to the positions of up to three microphones. The output of the these three microphones was recorded into three files in an ASCII format.   A sample input screen from this program can be seen in figure A.1.

Figure A.1. Sample of input screen from moving source simulation program.